INVESTIGATING THE EXPRESSION OF MUTATED PYRUVATE CARBOXYLASE OF *RHIZOBIUM ETLI* IN ACETYL COENZYME A BINDING SITE

KAMONMAN CHOOSANGTONG

A THESIS SUBMITTED IN PARTIAL FULFILLMENT
OF THE REQUIREMENTS FOR
THE DEGREE OF MASTER OF SCIENCE (BIOCHEMISTRY)
FACULTY OF GRADUATE STUDIES
MAHIDOL UNIVERSITY
2015

Thesis
entitled

INVESTIGATING THE EXPRESSION OF MUTATED PYRUVATE CARBOXYLASE OF *RHIZOBIUM ETLI* IN ACETYL COENZYME A BINDING SITE

……...
Miss Kamonman Choosangtong
Candidate

……...
Assoc. Prof. Sarawut Jitrapakdee,
Ph.D. (Molecular Biology)
Major advisor

……...
Prof. Pimchai Chaiyen,
Ph.D. (Biological Chemistry)
Co-advisor

……...
Asst. Prof. Auemphorn Mutchimwong,
Ph.D. (Air Quality Assessment)
Acting Dean
Faculty of Graduate Studies
Mahidol University

……...
Asst. Prof. Kittisak Yokthongwattana,
Ph.D. (Agricultural and environmental chemistry)
Program Director
Master of Science Program in Biochemistry
Faculty of Science
Mahidol University

Thesis
entitled

INVESTIGATING THE EXPRESSION OF MUTATED PYRUVATE CARBOXYLASE OF *RHIZOBIUM ETLI* IN ACETYL COENZYME A BINDING SITE

was submitted to the Faculty of Graduate Studies, Mahidol University
for the degree of Master of Science (Biochemistry)
on
June 30, 2015

……...
Miss Kamonman Choosangtong
Candidate

……...
Prof. Sakol Panyim,
Ph.D. (Biochemistry)
Chair

……...
Assoc. Prof. Sarawut Jitrapakdee,
Ph.D. (Molecular Biology)
Member

……...
Prof. Pimchai Chaiyen,
Ph.D. (Biological Chemistry)
Member

……...
Lect. Saowapa Duangpan,
Ph.D. (Plant breeding and plant genetics)
Member

……...
Asst. Prof. Auemphorn Mutchimwong
Ph.D. (Air Quality Assessment)
Acting Dean
Faculty of Graduate Studies
Mahidol University

……...
Prof. Skorn Mongkolsuk,
Ph.D. (Biological Science)
Dean
Faculty of Science
Mahidol University

ACKNOWLEDGEMENTS

This thesis would not have been possible unless it were contributions of many people. It is with immense gratitude that I acknowledge the support and help of my advisor, Assoc.Prof. Dr. Sarawut Jitrapakdee. His valuable guidance and advice throughout the course of my graduate study and research help me complete this thesis. I would like to appreciate Prof. Dr. Pimchai Chaiyen for her valuable suggestion. I would like to express my sincere gratitude to Prof. Paul Attwood for the opportunity and support me working in his laboratory at the School of Biomedical, Biomolecular and Chemical Science, University of Western Australia. His scientific advice and knowledge is so valuable that help me understand the work better. I would like to thank Miss Chutima Sereeruk for her generous help and teaching me all techniques in the lab during I worked in B315 lab. I would like to thank Dr. Abdussalam Adina-Zada and Mr. Chaiyos Sirithanakorn for their generous help and teaching me all techniques in the laboratory at the School of Biomedical, Biomolecular and Chemical Science, University of Western Australia. A special thanks to all other B315 lab members for advice and opinions on the lab-related issues and for precious friendships.

Lastly, I would like to thank my family for all their love and encouragement. For my parents and grandparents, their love and support is the most precious thing I have ever had in my life. I would like to dedicate this work to my dear father and grandfather; I hope you race in peace in the heaven.

Kamonman Choosangtong

INVESTIGATING THE EXPRESSION OF MUTATED PYRUVATE CARBOXYLASE OF *RHIZOBIUM ETLI* IN ACETYL COENZYME A BINDING SITE

KAMONMAN CHOOSANGTONG 5337217 SCBC/M

M.Sc. (BIOCHEMISTRY)

THESIS ADVISORY COMMIITTEE: SARAWUT JITRAPAKDEE, Ph.D. (BIOCHEMISTRY), PIMCHAI CHAIYEN, Ph.D. (BIOLOGICAL CHEMISTRY),

ABSTRACT

Pyruvate carboxylase (PC) is a biotin-dependent carboxylase enzyme catalysing the pyruvate carboxylation reaction to produce oxaloacetate with 2 partial reactions, MgATP-dependent carboxylation of biotin and the transfer of carboxyl group from carboxybiotin to pyruvate. PC is normally found as a tetramer with monomers of around 120-130 kDa in size. Each monomer contains 3 distinct functional domains which are biotin carboxylase (BC) domain, carboxyl transferase (CT) domain, and biotin carboxyl carrier protein (BCCP) domain. The recently found domain which mediates the tetramerization is PC tetramerization (PT) domain or allosteric domain. The previous study of residues in allosteric domain of PC from *Rhizobium etli* (RePC) (Arg427 and Arg472) indicated the important role of these residues in the allosteric regulation of PC. In this study, other residues in allosteric domain which directly interact with acetyl-CoA (Arg469 and Asp471) and indirectly interact with acetyl-CoA (Glu1027 and Asp1018) were examined the effects of these mutations on enzyme activity. R469S and R469K reduced the acetyl-CoA induced enzyme activity but less effect than R427 and R472 mutations. D471A completely destroyed the activity of enzyme activated by acetyl-CoA. E1027R caused decrease in enzyme activity induced by acetyl-CoA. All mutations increased in acetyl-CoA independent pyruvate carboxylation activity and ATP cleavage activity both in the presence and absence of acetyl-CoA. Results agree with previous studies that residues directly interacting with acetyl-CoA impact on the activation of enzyme by acetyl-CoA. Interaction between D1018 and R427 and the interaction between R469 and E360 only in subunit without acetyl-CoA bound support with previous studies that there is the transformation between the asymmetrical conformer and the symmetrical conformer during catalysis. Mutations of these residues may reduce the constraint of the enzyme and cause increase in catalytic activity in the absence of acetyl-CoA.

KEY WORDS: ACETYL-CoA/ ALLOSTERIC REGULATION/ RHIZOBIUM ETLI/ PYRUVATE CARBOXYLASE

88 pages

การศึกษาการแสดงออกของเอ็นไซม์ไพรูเวทคาร์บอกซิเลสที่กลายพันธุ์ของไรโซเบียม เอทิลิในตำแหน่งการจับของแอซิทิล โคเอ็นไซม์เอ

INVESTIGATING THE EXPRESSION OF MUTATED PYRUVATE CARBOXYLASE OF *RHIZOBIUM ETLI* IN ACETYL COENZYME A BINDING SITE

กมลแมน ชูแสงทอง 5337217 SCBC/M

วท.ม. (ชีวเคมี)

คณะกรรมการที่ปรึกษาวิทยานิพนธ์: ศราวุฒิ จิตรภักดี, Ph.D. (BIOCHEMISTRY), พิมพ์ใจ ใจเย็น, Ph.D. (BIOLOGICAL CHEMISTRY)

บทคัดย่อ

ไพรูเวทคาร์บอกซิเลสเป็นเอ็นไซม์ที่อาศัยไบโอตินซึ่งเร่งปฏิกิริยาเติมหมู่คาร์บอนให้ไพรูเวตเพื่อสร้างออกซาโลอะซิเตตด้วย 2 ปฏิกิริยาย่อยคือ การเติมหมู่คาร์บอนให้ไบโอตินโดยอาศัยแมกนีเซียมและการถ่ายหมู่คาร์บอนจากคาร์บอกซีไบโอตินไปยังไพรูเวท โดยปกติแล้วเอ็นไซม์อยู่ในรูปtetramerที่ประกอบด้วยmonomer ขนาด120-130 kDa แต่ละmonomerประกอบด้วย 3โดเมนที่ทำหน้าที่ต่างกันได้แก่ biotin carboxylase หรือBC โดเมน, carboxyl transferase หรือCTโดเมนและ biotin carboxyl carrier protein หรือBCCPโดเมน โดเมนที่เพิ่งถูกพบซึ่งช่วยในการ tetramerization เรียกว่า PC tetramerization โดเมน, PT โดเมน, หรือ allosteric โดเมน การศึกษาของresidue ใน allosteric โดเมนของไรโซเบียม เอทิลิ (RePC)ได้แก่อาร์จินีน427และอาร์จินีน472 บ่งชี้ถึงหน้าที่สำคัญต่อการควบคุมแบบอะโลสเตอริก(allosteric regulation)ของเอนไซม์ ในงานวิจัยนี้ได้ศึกษาresidueตัวอื่นในallostericโดเมนที่จับกับแอซิทิลโคเอ็นไซม์เอโดยตรงได้แก่อาร์จินีน469และแอสพาเตท471และทางอ้อมได้แก่กลูตาเมท1027และแอสพาเตท1018ในผลของการกลายพันธุ์ต่อการทำงานของเอ็นไซม์ R469Sและ R469Kลดการทำงานของเอ็นไซม์เมื่อถูกกระตุ้นโดยแอซิทิลโคเอ็นไซม์เอแต่ไม่มากเท่าR427และR472ที่กลายพันธุ์ D471Aได้ทำลายการทำงานของเอ็นไซม์เมื่อถูกกระตุ้นโดยแอซิทิลโคเอ็นไซม์เอ E1027Rลดการทำงานของเอ็นไซม์เมื่อถูกกระตุ้นโดยแอซิทิลโคเอ็นไซม์เอ เอ็นไซม์ที่กลายพันธุ์ทุกตัวเพิ่มการทำงานของเอ็นไซม์เมื่อไม่มีแอซิทิลโคเอ็นไซม์เอและเพิ่มการสลายเอทีพีทั้งที่มีและไม่มีแอซิทิลโคเอ็นไซม์เอ ผลการทดลองได้สนับสนุนการศึกษาก่อนหน้านี้ว่า residueที่จับกับแอซิทิลโคเอ็นไซม์เอโดยตรงมีผลต่อการทำงานของเอ็นไซม์เมื่อถูกกระตุ้นโดยแอซิทิลโคเอ็นไซม์เอ การจับกันของD1018กับR427และR469กับE360ในหน่วยย่อยของเอ็นไซม์ที่ไม่มีแอซิทิลโคเอ็นไซม์เอจับเท่านั้นสนับสนุนการศึกษาก่อนหน้านี้ว่าเอ็นไซม์มีการเปลี่ยนโครงสร้างจากอสมมาตรไปเป็นสมมาตรระหว่างเกิดปฏิกิริยา การกลายพันธุ์ของresidueเหล่านี้อาจไปลดการควบคุมการทำงานของเอ็นไซม์ทำให้เพิ่มการทำงานของเอ็นไซม์เมื่อไม่มีแอซิทิลโคเอ็นไซม์เอ

88 หน้า

CONTENTS

CONTENTS (cont.)

LIST OF TABLES

LIST OF FIGURES

LIST OF FIGURES (cont.)

LIST OF FIGURES (cont.)

LIST OF ABBREVIATIONS

Abbreviations used throughout this thesis are listed below.

ACC	=	acetyl-CoA carboxylase
ATP	=	adenosine tri-phosphate
ATP-γ-S	=	adenosine 5'-O-(3-thiotriphosphate)
BC	=	biotin carboxylase
BCCP	=	biotin carboxyl carrier protein
BSA	=	bovine serum albumin
CoA	=	coenzyme A
CT	=	carboxyltransferase
DTE	=	dithioerythritol
DTT	=	dithiothreitol
EDTA	=	ethylenediaminetetraacetic acid
h	=	Hill coefficient or cooperativity parameter
HsPC	=	human pyruvate carboxylase
IPTG	=	isopropyl-β-D-thiogalactopyranoside
K_a	=	activation constant
k_{cat}	=	the apparent first-order rate constant
k^0_{cat}	=	the apparent first-order rate constant at zero acetyl-CoA
LmPC	=	*Listeria monocytogenes* PC
MDC	=	methylmalonyl-CoA decarboxylase
ODC	=	oxaloacetate decarboxylase
PC	=	pyruvate carboxylase
PCC	=	propionyl-COA carboxylase
PMSF	=	phenylmethylsulphonyl fluoride
PT	=	PC tetramerization

LIST OF ABBREVIATIONS (cont.)

RePC	=	*Rhizobium etli* pyruvate carboxylase
SaPC	=	*Staphylococcus aureus* pyruvate Carboxylase
SDS-PAGE	=	sodium dodecyl sulphate polyacrelamide gel electrophoresis
TEMED	=	N,N,N', N'-tetramethylethylethylenediamine
Tris	=	tris-(hydroxymethyl)methylamine

CHAPTER I
INTRODUCTION

1.1 Biotin-dependent enzymes

Biotin, vitamin H (figure 1.1) is a cofactor of several enzymes involving in various metabolic pathways including gluconeogenesis, lipogenesis, amino acid degradation and odd chain fatty acid degradation. Biotin serves as a carboxyl carrier by transferring the carboxyl group from donor to an acceptor substrate in carboxylation, decarboxylation, and transcarboxylation reactions (9).

The reaction catalyzed by biotin-dependent enzymes is divided into two steps. The first step involves the carboxylation of biotin to form carboxybiotin. The second step is the transfer of carboxyl group from carboxybiotin to an acceptor molecule to form the carboxylated product. The biotin molecule which is covalently attached to the enzyme, acts as a mobile molecule that swings between two different active sites of the enzyme. According to these reaction mechanisms, biotin-dependent enzymes consist of three functional domains, namely, the biotin carboxylase or BC domain, the carboxyltransferase or CT domain, and the biotin-carboxyl carrier protein or BCCP domain.

1.1.1 Carboxylase (1)

Carboxylase is one of enzyme group catalyzing the carboxylation reaction. In this reaction, biotin attached to enzyme is carboxylated from bicarbonate (carboxyl donor) to form carboxybiotin intermediate in the presence of ATP and Mg^{2+} in the first partial reaction. Then, in the second partial reaction, the carboxyl group from carboxybiotin is transferred to an accepter molecule. The following scheme shows how the carboxylation reaction occurs (1):

$$\text{Enzyme-biotin} + \text{ATP} + HCO_3^- \longrightarrow \text{Enzyme-biotin-}CO_2^- + \text{ADP} + \text{Pi} + H^+$$

$$\text{Enzyme-biotin-}CO_2^- + \text{R-H} \longrightarrow \text{Enzyme-biotin} + \text{R-}CO_2^-$$

These two partial reactions occur at separate active sites. Therefore the carboxylase contains three functional domains: The biotin carboxylase domain or BC domain catalyzes the carboxylation of biotin. The carboxyltransferase or CT domain catalyzes the transfer of carboxyl group from biotin to acceptor molecule. The third component is the biotin-carboxyl carrier protein or BCCP domain where the biotin is covalently attached and swings between two active sites of BC and CT domains, allowing the reaction to complete. The biotin-dependent carboxylases include acetyl-CoA carboxylase (ACC), pyruvate carboxylase (PC), propionyl-CoA carboxylase (PCC), β-methylcrotonyl-CoA carboxylase (MCC), geranyl-CoA carboxylase (bacterial enzyme), and urea carboxylase (bacterial enzyme).

1.1.2 Decarboxylase (1)

This enzyme catalyzes the decarboxylation reaction. It facilitates the transport of Na^+ across membrane in anaerobes to produce Na^+ gradient concomitant with the production of ATP. Biotin-dependent decarboxylases include oxaloacetate decarboxylase (ODC), methylmalonyl CoA decarboxylase (MDC), and glutaconyl-CoA decarboxylase (GDC). This following scheme shows decarboxylation reaction (1).

$$RCO_2^- + H_2O + 2Na^+_{\text{intracellular}} \longrightarrow RH + HCO_3^- + 2Na^+_{\text{extracellular}}$$

1.1.3 Transcarboxylase

Transcarboxylase is the enzyme which catalyzes the transcarboxylation reaction, coupling two carboxylation reactions. There is only one member which is the transcarboxylase from *Propionibacterium shermanii*. It transfers carboxyl group from methylmalonyl-CoA to pyruvate yielding propionyl-CoA and oxaloacetate. This following scheme shows transcarboxylation reaction (1).

$$RCO_2^- + R'H \longrightarrow RH + R'CO_2^-$$

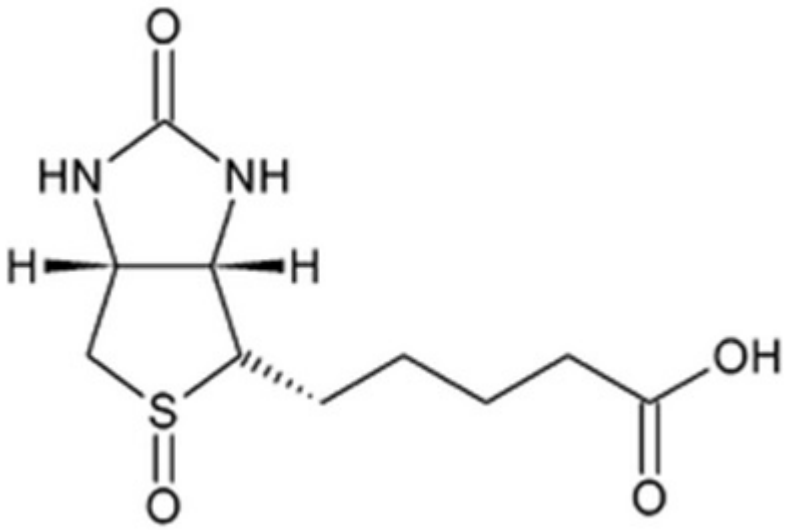

Figure 1.1 Structure of biotin. Biotin consists of two five member rings (ureido and tetrahydrothiophene rings) fused cis to one another. Extending from the tetrahydrothiophene ring is a valeric acid side chain which is in *cis* configuration, with respect to the ureido ring. Biotin contains three chiral carbon atoms leading to eight stereoisomers, but there is only one isomer described above which is biologically active (2, 3).

1.2 Pyruvate carboxylase (PC)

Pyruvate carboxylase or PC is a biotin-dependent carboxylase enzyme which catalyzes the carboxylation of pyruvate to produce oxaloacetate. Since oxaloacetate, the product from this reaction is one of the intermediates in Krebs cycle. As oxaloacetate is being used in various biosyntheses (4), this reaction is considered to be an anaplerotic reaction which refills TCA cycle intermediate pools. PC is found in many organisms including archea bacteria and eukaryotes.

1.2.1 PC in microorganisms

Pyruvate carboxylase is widely found in many prokaryotes such as *Pseudomonas, Bacillus, Rhizobium, Mycobacterium, Stapphylococcus*, and archea. However, it is not found in enterobacteriaceae which uses phosphoenolpyruvate carboxylase to produce oxaloacetate directly from phosphoenolpyruvate(5,6). PC in yeast is found in two isoforms, PYC1 and PYC2, expressed by separate genes. The regulation of these genes are affected by growth phase, carbon, and nitrogen sources especially ammonium ion (7, 8).

1.2.2 PC in mammals

PC in mammals is tissue-specifically expressed with different levels depending on tissue type. In liver and kidney, PC catalyzes the first committed step of gluconeogenesis to produce oxaloacetate which is subsequently converted to glucose in this pathway. In adipocytes, PC is involved in the supply of acetyl group in the form of citrate for *de novo* fatty acid synthesis, as well as involving in glyceroneogenesis, a pathway that produce glycerol for fatty acid re-esterification. In pancreatic beta cells, PC is important for glucose-induced insulin secretion. While in astrocytes, PC is required for *de novo* synthesis of glutamate, an important excitatory neurotransmitter supplied to astrocytes.(9) (Figure1.2)

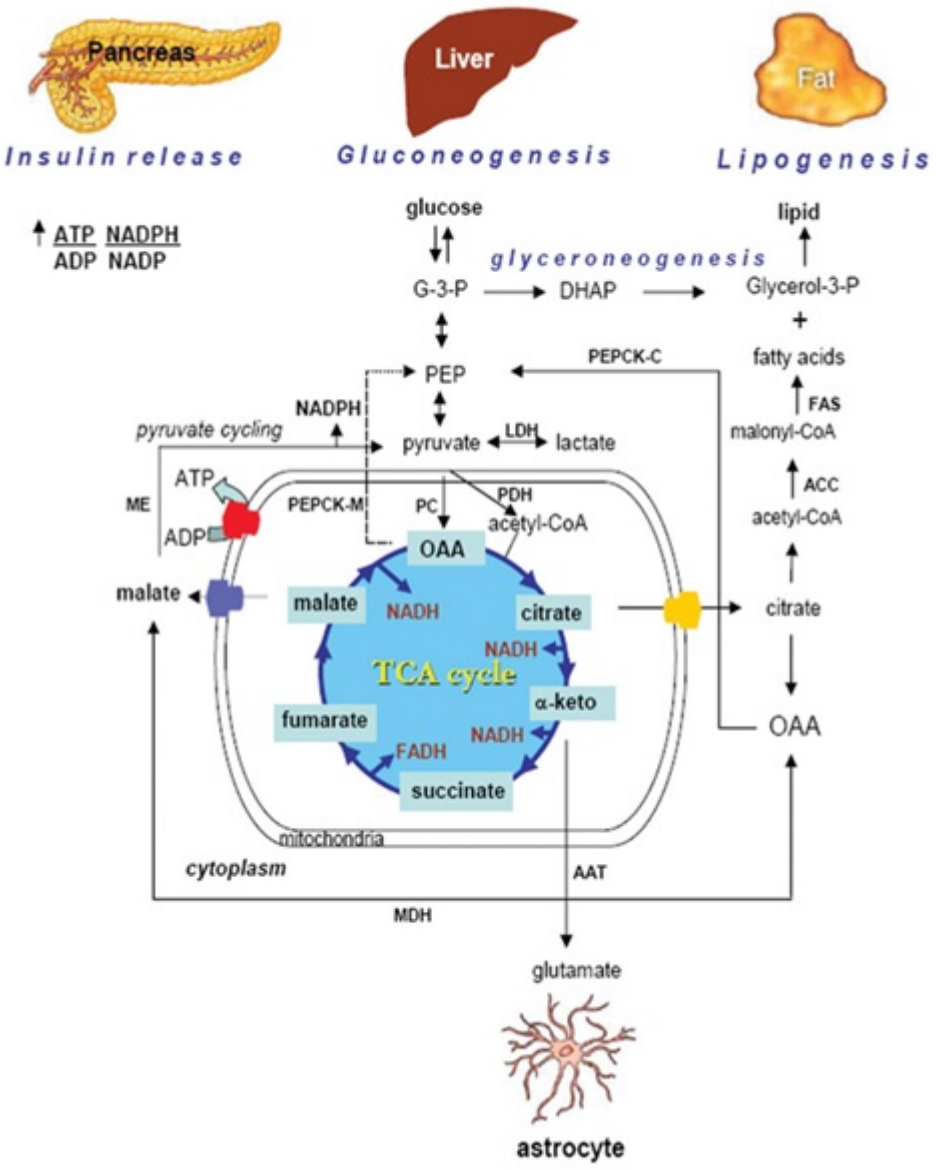

Figure 1.2 The anaplerotic functions of PC in mammalian tissues. Four major biosynthetic pathways are shown: gluconeogenesis in liver and kidney, lipogenesis and glyceroneogenesis in adipocytes, insulin secretion in pancreatic beta cells, and synthesis of excitatory neurotransmitter in astrocytes (9).

1.3 The catalytic mechanism of pyruvate carboxylase

The carboxylation of pyruvate to produce oxaloacetate catalyzed by pyruvate carboxylase consists of two steps as follows;

$$\text{Enzyme-biotin} + \text{ATP} + HCO_3^- \xrightarrow[Mg^{2+}]{\text{Acetyl-CoA}} \text{Enzyme-biotin-}CO_2^- + \text{ADP} + \text{Pi} + H^+$$

$$\text{Enzyme-biotin-}CO_2^- + \text{pyruvate} \longrightarrow \text{Enzyme-biotin} + \text{oxaloacetate}$$

The first partial reaction is the carboxylation of biotin from bicarbonate as a carboxyl donor. In this step, it also requires ATP and Mg^{2+}. ATP activates bicarbonate to form a carboxyphosphate intermediate which is quite difficult to directly observe because of the short estimated half-life (10) (Fig 1.3A). Nevertheless the formation of this intermediate was evidenced by the observation of an exchange of ^{18}O between $HC^{18}O_3$ and Pi in reactions catalyzed by propionyl-CoA carboxylase and biotin carboxylase, suggesting the interaction between bicarbonate and γ-phosphate of ATP (11, 12). This proposed mechanism was further supported by the finding that pyruvate carboxylase is able to catalyze the phosphorylation of ADP in the presence of carbamyl phosphate, an analog of carboxyphosphate (10).

The carboxyphosphate intermediate carboxylates biotin at 1'-N position either directly or pass through the decarboxylation, releasing CO_2, which in turn acts as a carboxylating agent (Fig 1.3B). The carboxylated position of biotin suggests the essential of biotin to exist in an enol form so that 1'-N position is sufficiently nucleophilic. According to several studies, the stabilization of the enolate oxygen of the enol form of biotin is relevant to a cysteine-lysine ion pair. A scheme was proposed that the lysine ε-amino group deprotonates the sulphydryl of the cysteine.The thiolate deprotonates the 1'-N of biotin while the ε-NH^+_3 stabilizes the enolate oxygen of the enol form of biotin (13, 14, 15).

Jitrapakdee *et al.* (16), when comparing the sequences of several PC with the crystal structure of the biotin carboxylase subunit of *E. coli* acetyl-CoA carboxylase determined by Waldrop *et al*. (17), noted that C230 and K238 located in the active site of biotin carboxylase subunit, are sufficiently close to allow their cross-linking. These two residues are also strictly conserved in all biotin-dependent carboxylases. Nevertheless, mutation of this cysteine to alanine of acetyl-CoA

carboxylase from *E. coli* showed that C230 is not important for the biotin carboxylation. The result from this mutation showed 50-fold increase in the K_m for MgATP, suggesting a role of this residue in ATP binding. From Kazuta *et al*. (18), K238 mutation caused many fold increase in the K_m for ATP. Mutation of K238 to K238Q caused enzyme fail to carboxylate free biotin, so K238 may be relevant to the stabilization of enolate oxygen of biotin.

Recently, the structure of PC from *Rhizobium etli* (RePC) reveals several interacting residues in the BC subunit from ACC. For example, Lys245 interacts with the γ-phosphate of ATP. G297, and Asn299, previously unrecognized residues, are essential for coordinating the two essential Mg^{2+} ions and ATP binding (Fig 1.4).

In the second partial reaction, carboxyl group from carboxybiotin is transferred to pyruvate to produce oxaloacetate. From the pH profile and kinetic isotope effect studies on the oxamate-induced decarboxylation of oxaloacetate (16, 20) suggests the relevance of a cysteine-lysine ion pair in enolisation of biotin at the site of transcarboxylation reaction. Nevertheless, cysteine residue is not highly conserved in this part of PC.

The study of crystal structures of 5s subunit of transcarboxylase from *P. shersermanii* (21) reveals mechanistic insights into PC since the 5s subunit of this enzyme is functionally and sequentially homologous to the C-terminal CT region of PC. They found the unexpected carbamylated Lys184 located near the pyruvate binding site and coordinated to the active-site cobalt. This Lys184 residue was not carbamylated and formed a hydrogen bond with Cys154 in the presence of oxaloacetate. Moreover, in the 5S-pyruvate complex, the Lys184 was found to be in two chemical and conformational forms, the non-carbamylated and carbamylated forms. These structures suggest that carbamylated Lys184 might be essential for the carboxyl transfer from carboxybiotin to pyruvate. The proposed mechanism was determined by mutation of Lys184. The mutant was catalytically inactive which verified the essential role of Lys184 in transcarboxylation reaction. The similar results from mutation of corresponding lysine residue in PC from *B. therodenitrificans* (Lys712) were received. Nevertheless, the mutation results from the corresponding lysine residue in RePC (Lys718) (26) retained only 4% specific activity of enzyme. Therefore, this lysine residue is not completely essential for PC catalysis. The Cys154,

another residue in the 5s subunit study is also mutated and studied but mutation in this residue still maintained approximately 50% of activity of wild-type. In addition, this cysteine is not conserved in all PCs.

The study from Yong-Biao *et al.* (22) which mutated these following highly conserved residues in PCs and in 5S: Asp762, Asp713, Glu576, Glu592, Asp543, and Asp649. The D762N mutation had small effect on the transcarboxylation reaction. The D713N, E576Q, and E592Q affected the stability of tetrameric conformation rather than the overall reaction. The D543E mutation retained 4.7% of the wild-type activity. The K_m^{pyruvate} of this mutant was 54-fold higher than that of the wild-type. The D649N mutation retained 2% of the wild-type activity. These D543E and D659N mutations also affected the oxamate-induced oxaloacetate decarboxylation reaction by reducing 4.5- and 14-fold in specific activity respectively and slightly changing in the K_ms for oxaloacetate and oxamate. In addition, Yong-Biao *et al.* (22) suggested a mechanism by which Asp543 primarily acts as a base to deprotonate pyruvate to form enolate. The positioning of the ε-NH_3^+ of Lys712 adjacent to the ureido oxygen of carboxybiotin then induces its decarboxylation and subsequent carboxylation of the enol form of pyruvate. The Asp543 protonates the 1'-N of biotin to return it to the keto form. The carboxy group of Asp649 acts as a ligand to the metal ion, positioning it adjacent to the carbonyl oxygen of pyruvate to facilitate enolization. The corresponding aspartate residues in transcarboxylase 5S are Asp23 and Asp127 respectively and those in RePC are Asp549 and Asp655. The carboxy group of Asp23 is shown to be a ligand of the cobalt ion in 5S and is 5.6 Å from the methyl carbon of pyruvate. Asp549 in RePC is also a ligand of the bound metal ion (zinc). The carboxy groups of Asp127 and Asp 655 are 16 Å from the bound metal ion and Asp127 is 12 Å from the methylene carbon of pyruvate. Thus the assumed roles of Asp543 and Asp469 in the proposed mechanism of Yong-Biao *et al.* (22) are not supported by the structures of 5S and RePC.

Structural determination of *Staphylococcus aureus* PC (SaPC) and human PC (hPC) were found that the BCCP domain of both enzymes were bound to pyruvate and buried in the CT active site. The Thr908 in hPC and the corresponding Thr876 in SaPC are located between pyruvate and biotin and form hydrogen bond with 1'-N

biotin (Fig. 1.6). Mutation of this Thr822 in RePC inactivated the forward pyruvate carboxylating and the reverse oxaloacetate decarboxylating activities (23). Nevertheless, ADP phosphorylating and ATP cleavage activity of this mutation did not change. Zeczycki et al. (23) proposed that the carboxyltransfer mechanism occurs through hydrogen-bonding interaction with Thr882.

From the structure of 5S bound to pyruvate, Arg22 and Gln26 can form hydrogen bonds with the oxygen of carbonyl group. (21) It reveals the role in promoting enolisation of pyruvate as a prelude to carboxylation in the forward reaction and promoting decarboxylation of oxaloacetate in the reverse reaction. The corresponding Arg and Gln are highly conserved in PCs including RePC (21). Duangpan et al. (24), mutated Arg548 and Gln552, residues in the CT active site and showed that these mutants could not catalyze full reaction of biotin-dependent decarboxylation of oxaloacetate. However, the mutants retained the ability to catalyze bicarbonate-dependent ATP cleavage and ADP phosphorylation by carbamoyl phosphate reactions occurred in the active site of the BC domain. This indicates that Arg548 and Gln552 facilitates pyruvate binding and subsequent proton transfer between pyruvate and biotin in the partial reaction catalyzed in the active site of the CT domain in RePC.

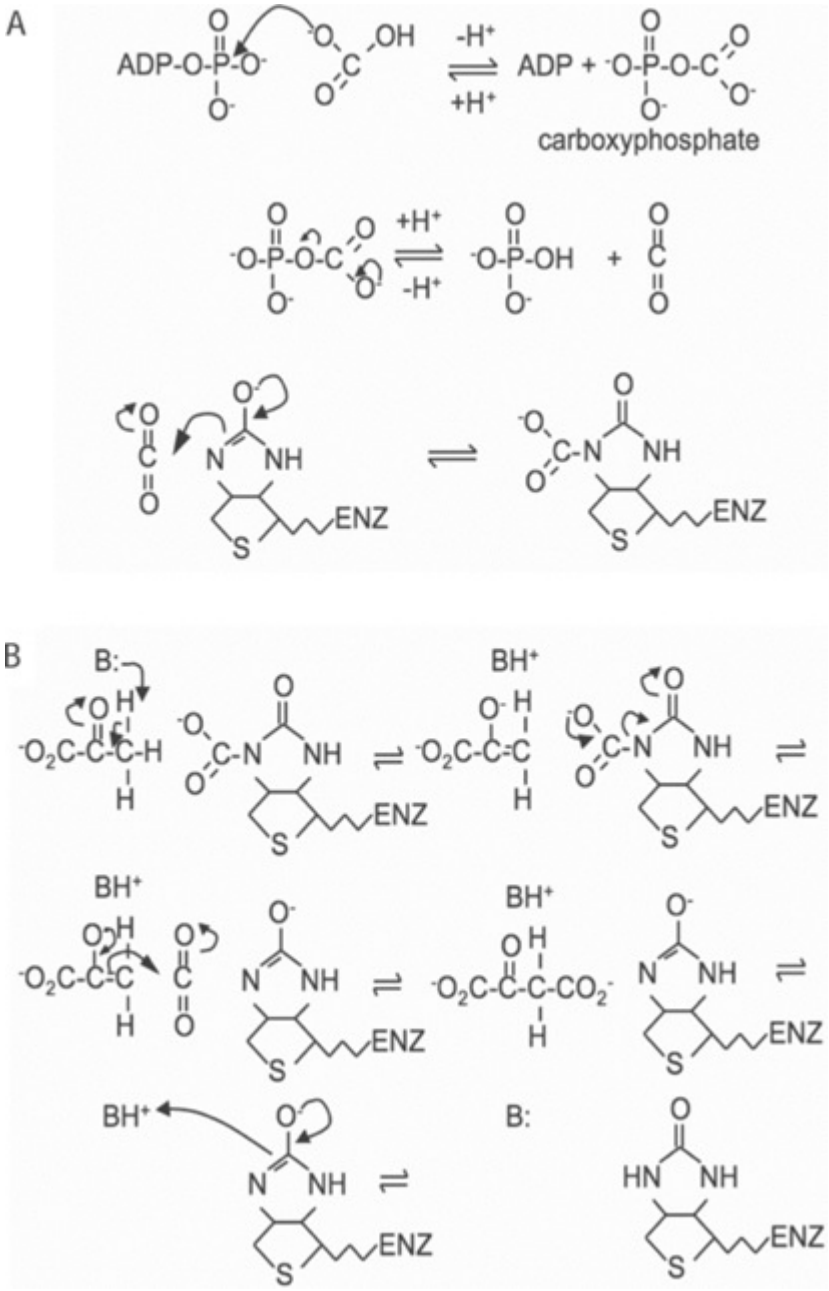

Figure 1.3 The carboxyphosphate intermediate formation. (A) Chemical mechanism for the biotin carboxylation via a carboxyphosphate intermediate. (B) Chemical mechanism for the pyruvate carboxylation by carboxybiotin. B represents the basic residues located in the enzyme active site (9).

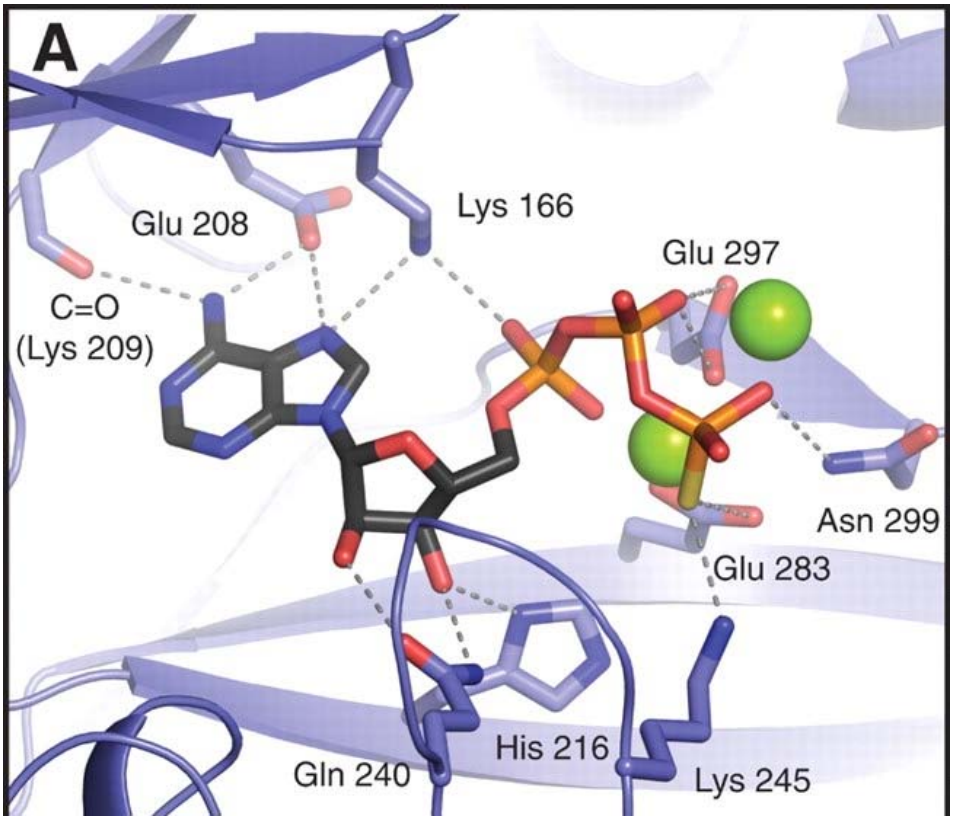

Figure 1.4 The ATP binding site of RePC. There are several residues not previously noted in the structure of the BC subunit from ACC (19).

1.4 The structure of pyruvate carboxylase

Pyruvate carboxylase is found in the organism in two different forms, α_4 and $\alpha_4\beta_4$. In α_4 form (5, 25), PC consists of four identical subunits, approximately 120-130 kDa in size. This form is found in most organisms ranging from bacteria, fungi, and invertebrates to vertebrates. In $\alpha_4\beta_4$ form which consists of two polypeptide chains in one subunit, ~55 kDa non-biotinylated polypeptide (α) which possesses BC activity and ~70 kDa biotinylated polypeptide (β) possessing CT activity. This form is found in archaea bacteria such as *Methanobacterium* sp., *Methanococcus* sp., and *Methanosarcina* sp. (26, 27), and certain bacteria such as *Aquifex aeolicus* (28) and *Pseudomonas* sp (29, 30). Most α_4 PCs are subject to allosteric regulation: Acetyl-CoA is an activator for PC while L-aspartate is an inhibitor of it. However, $\alpha_4\beta_4$ PC activity is completely independent from acetyl-CoA (26, 27, and 31).

PC of *Rhizobium etli* (RePC) is in α_4 form which consists of four identical subunits. Each subunit is a 120 kDa single polypeptide chain containing 3 domains; biotin carboxylase domain or BC, carboxyl transferase domain or CT, and biotin-carboxyl carrier protein domain or BCCP. St Maurice et al. (19) have also identified the fourth domain, namely, the allosteric domain in which acetyl-CoA binds (Figure 1.6). This allosteric domain contains two separate parts of the polypeptide chain. The first part includes residue 471-488 which folds to a central α helix while the second part including residue 1002 -1073 folds to 4 antiparallel β strands bracketing a central α helix (Figure 1.6).

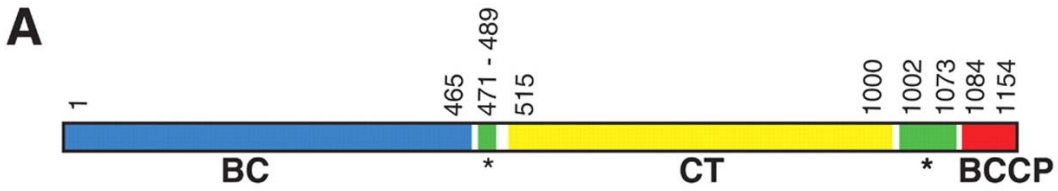

Figure 1.5 The single polypeptide chain of Pyruvate carboxylase from *Rhizobium etli* (RePC) containing 3 domains: biotin carboxylase (BC) appeared in blue, carboxyl transferase (CT) appeared in yellow, and biotin-carboxyl carrier protein (BCCP) appeared in red, and recently found domain, the allosteric domain for binding with acetyl-CoA appeared in green (19).

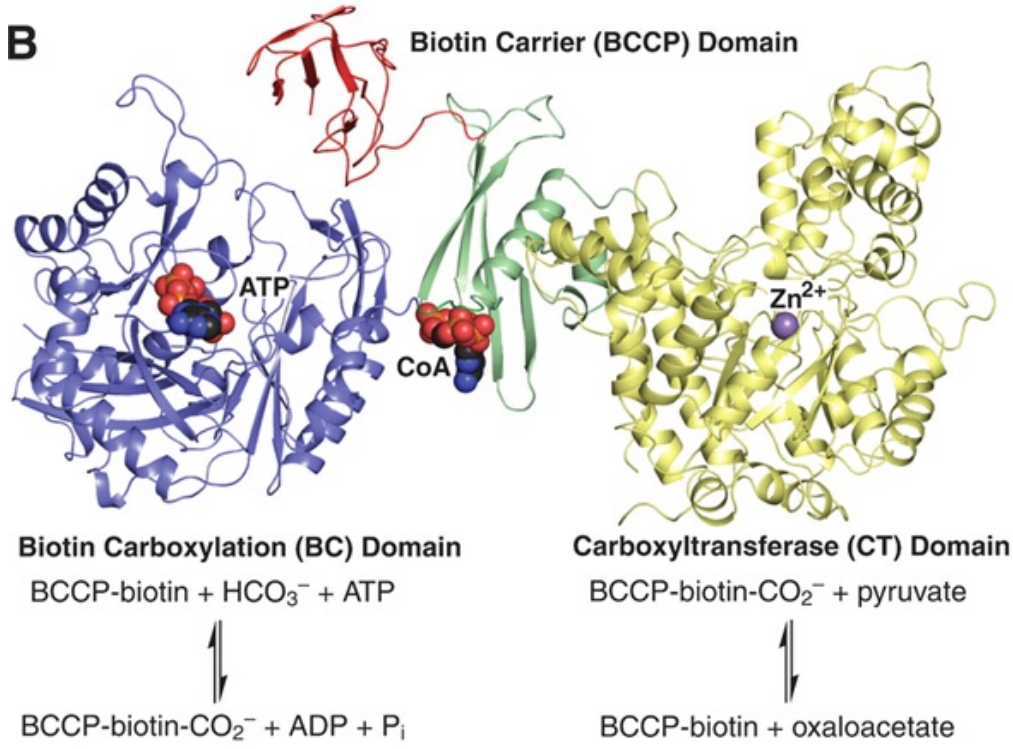

Figure 1.6 The three-dimensional diagram showing the arrangement of 4 domains from 1 single polypeptide chain of RePC (19).

1.4.1 The structure of BC domain

Biotin carboxylase or BC domain is part of biotin-dependent enzyme where the first partial reaction or the biotin carboxylation, occurs. This domain is highly conserved within biotin-dependent enzyme members. From the studies of complete crystal structure of *Rhizobium etli* and *Staphylococcus aureus* andstudies of separated BC domain of PC from *Aquifex aeolicus* (28), BC domain of PC from *Bacillus thermodenitrificans* (41), and ATP-bound subunit of ACC from *Escherichia* coli show that BC domain has three subdomains which are A, B, and C including AB linker which links between subdomain A and B (Fig1.6). Subdomain A, C and AB linker form the cylindrical structure where the ATP biding pocket or the active site of BC domain located in top of this structure, while B subdomain structures as a hinged lid closing this ATP binding site. Subdomain B is stimulated to close and moved approximately 45º relative to subdomain A and C when ATP binds with BC domain (42). A closed conformation of subdomain B is found in the ATP-bound BC domain of *Staphylococcus aureus* PC (SaPC), however, large differences can be observed when compared to those of *E.coli* acetyl-CoA carboxylase (49).

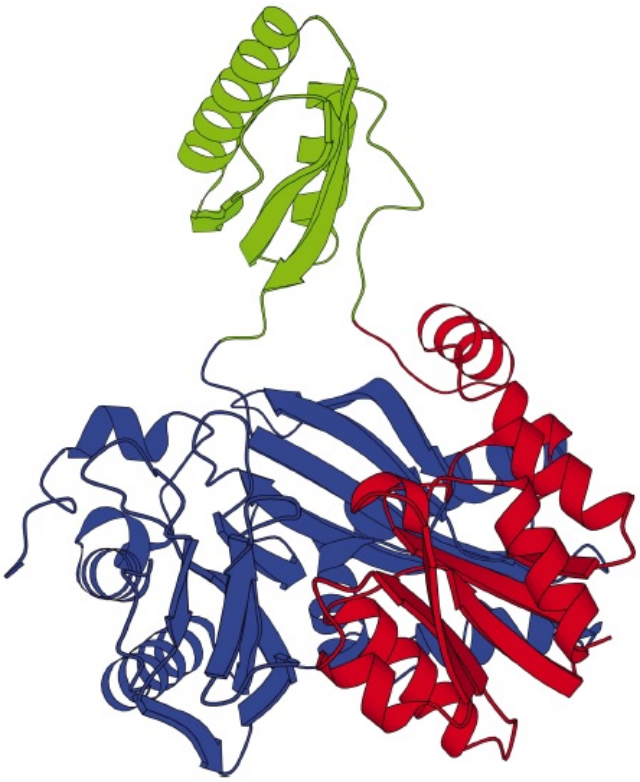

Fig 1.7 The overall schematic structure of BC subunit of Pyruvate carboxylase (PC-β) from *Aquifer aeolicus* showing 3 domains; domain A in red, domain B in green, and domain C in blue color (28).

1.4.2 The structure of CT domain

The carboxyl transferase or CT domain is the region where the second partial of reaction occurs. There is carboxyl transfer from carboxybiotin to pyruvate to produce oxaloacetate. Structural studies of CT domain of two biotin-dependent and pyruvate-binding enzymes, the 5S subunit of transcarboxylase (5s) and the α-subunit of oxaloacetate decarboxylase (α-OAD), show that they are structurally homologous to CT domains of RePC, SaPC, and hPC(5). The CT domain is composed of a core α8β8 TIM barrel located at N-terminal and a funnel, a C-terminal subdomain, which leads a metal ion binding at the mouth of the TIM barrel. The center of transcarboxylation reaction of these biotin-dependent enzymes is defined as a conserved position at the mouth of the TIM barrel due to reported structures of the homologous CT domains (5). However, the central metal ion is varied between species. For example, Zn^{2+} is suggested as an active-site metal ion of RePC (5) while $Co^{2+}$is an active site metal ion of 5s subunit of transcarboxylase (22). Nevertheless, the exact identity of an active-site metal ion of SaPC is unknown. (5).The metal ion of PC is coordinated by pyruvate, a conserved aspartate residue, two conserved histidine residues, and a conserved carbamylated lysine residue. Those residues are exactly analogous residues to the metal-ion binding site found in the active site of 5s transcarboxylase (5). A dramatic decrease or complete loss of catalytic activity in PC is caused by mutation of metal binding residues. The new insight into the molecular basis given from the structures of pyruvate and biotin bound hPC and SaPC in the CT domain shows that enzyme dysfunction from mutation is involved in human PC deficiencies (5). For example, M743I mutation is located near the pyruvate-binding site and A610T mutation is located in the biotin-binding site. The abolished catalytic activity of PC from A610T mutant SaPC is caused by blocking biotin binding to the CT active site (50).

1.4.3 The structure of BCCP domain

From the X-ray crystallographic studies of the BCCP subunit of *Escherichia coli* ACC and BCCP domain from the 1.3s subunit of *Propionibacterium shermanii* transcarboxylase reveals that they share structural similarity with the BCCP domain from hPC, RePC and SaPC (46). The BCCP domain is a flattened β-barrel structure comprising 2 four-stranded β-sheets, interrupted by a structural loop forming

a structure so called thumb.

The biotin prosthetic group is covalently attached to a specific lysine in thumb structure. The BCCP domain of RePC transfers the tethered biotin cofactor between the two active sites of BC and CT domain, located in opposing polypeptide chains (48). The studies of SaPC structure and the C-terminus of hPC both exhibits the position of biotin which projects away from BCCP and is located in proximity to pyruvate in the CT active site (5). In hPC and SaPC, their BCCP domain and biotin shares similar conformation which supports their biologically relevant conformation (5, 49).

1.4.4 The structure of allosteric domain

Recent study from the X-ray crystallography of RePC has discovered the role of the central structural domain of PC in binding with the allosteric activator, acetyl-CoA and influencing the orientation and arrangement of individual domains of PC. This central domain has called the allosteric domain as the fourth domain (48). This domain is unique to PC because it shares no sequence similarity with other biotin-dependent enzymes. The structure of this domain consists of a central α-helix and four antiparallel β-strands bracketing the helix (Fig 1.5.2). The first part, a central α-helix, is located in the N-terminal of polypeptide chain. It links between BC and CT domains. The second part which is in the C-terminal segment folds around the central α-helix as antiparallel (β_4) sheet connecting the CT and BCCP domain. The study of crystal PC from *Rhizobium etli* showed the asymmetrical tetramer which proposed the activating mechanism of enzyme by acetyl-CoA. Acetyl-CoA binding reduced distance between active sites of BC and CT domains from 80 Å to 65 Å of a dimer pair while the distance between these two active sites of another dimer pair is too far to perform catalysis (19). This supports the half-site reactivity of PC enzymes.

Xiang et al. 2008. reveal the new domain important for tetramerization so called the PC tetramerization or PT domain. This domain consists of two segments on one polypeptide chain. The first segment is located between BC and CT domains forming an α-helix, and the second part is located between CT and BCCP domains forming four-stranded antiparallel β-sheet (Fig. 1.8) (48). The location, orientation, and role in tetramerization are similar to the allosteric domain in RePC (Fig.1.9) (19).

The crystal structure of HsPC (only missing BC domain) reveals that the tetramer of human CT+PT+BCCP domain is made up of two dimers (48). The CT domain of each monomer begins folding at TIM barel to form dimer (48). Then two PT domains at the interface of one dimer interact with their equivalents in another dimer to form tetramer (48). There are two residues making the largest distribution in this interface which are Phe1077 and Leu1084 (48). Xiang et al. 2008 have studied role of Phe1077 by performing site-directed mutagenesis to alanine and glutamic acid and found that mutations disrupted tetramerization demonstrating the importance of this domain in subunit assembly (Fig.1.8d) (48).

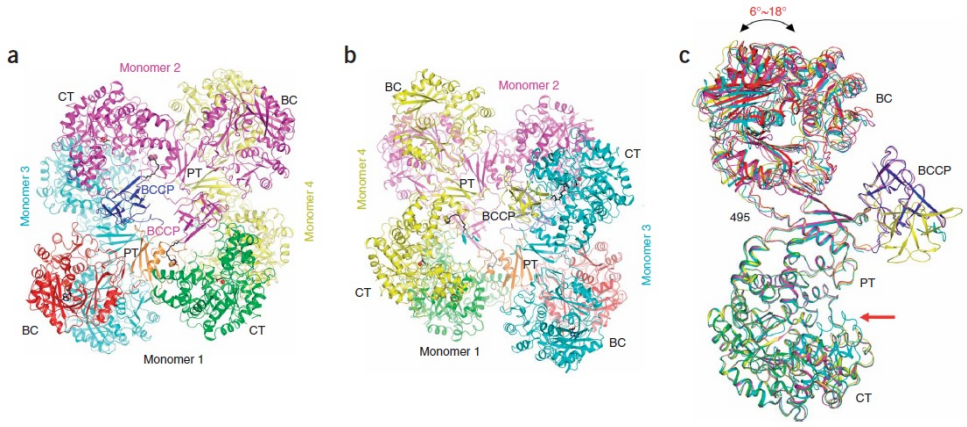

Figure 1.8 The schematic drawing of SaPC tetramer in complex with CoA. In the top layer, the monomer 1 given in separated color; BC in red, CT in green, BCCP in blue, and PT in gold. The CoA molecule was shown as a black space-filling model. Monomer 2, 3, and 4 were shown in magenta, cyan, and yellow respectively. The gray highlighted circle showed one of CoA binding site (a). The schematic drawing of the bottom layer of the tetramer of CoA complex with SaPC (b). The structural overlay of all four monomers of CoA complexed with SaPC based on its CT domain. The BC domain shows 6˚ difference in their relative orientation (c) (48).

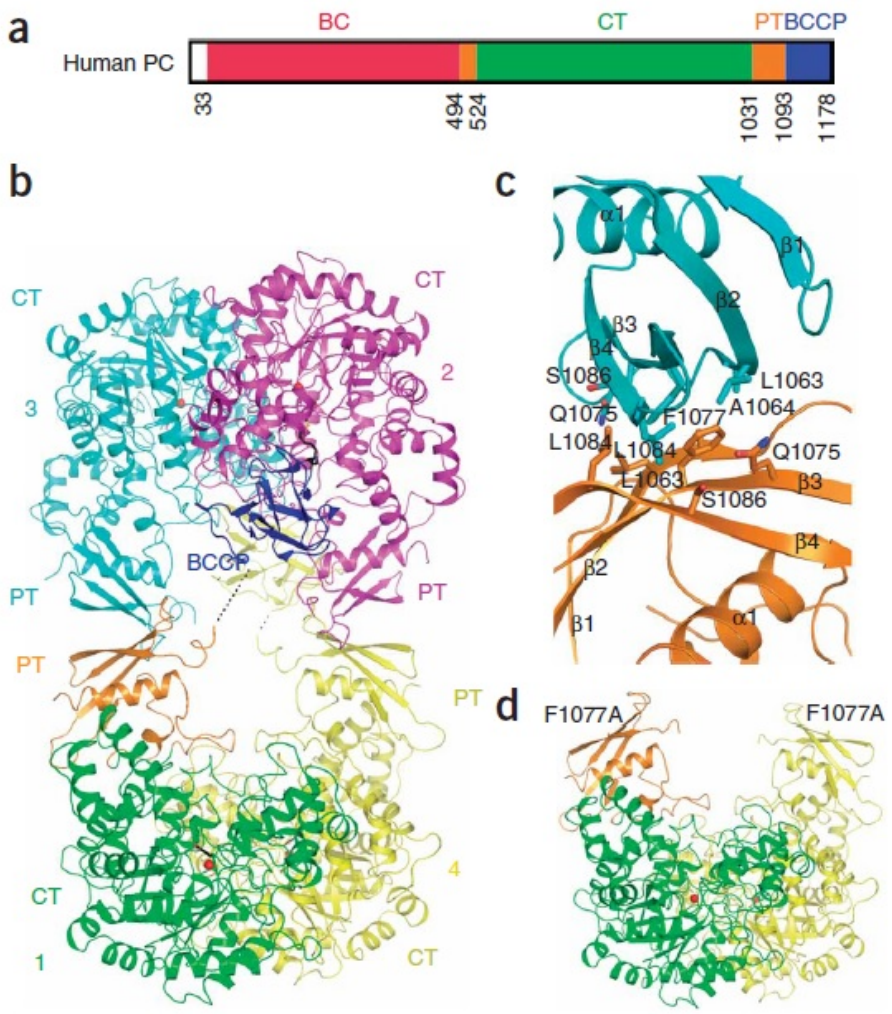

Figure 1.9 The schematic drawing shows domain organization of human PC: red is BC, green is CT, blue is BCCP, and orange is PT domain (a). Schematic drawing shows CT+PT+BCCP domain tetramer of human PC. Each domain of monomer 1 is given color similar to domain color in panel a while monomers 2, 3 and 4 are shown in color magenta, cyan, and yellow respectively (b). Schematic drawing shows detailed interactions between PT domain of monomer 1(orange) and PT domain of monomer 3(cyan) in the tetramer interface of human PC (c). Schematic drawing shows the dimer of CT+PT+BCCP domain of F1077A from HsPC (d). (48)

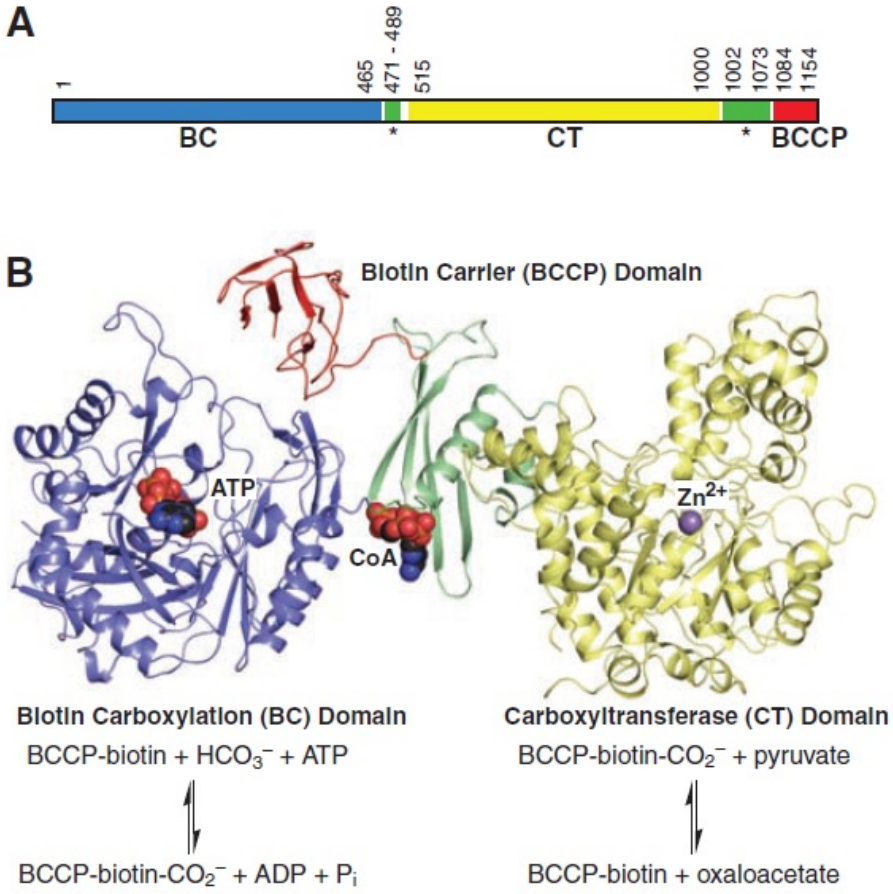

Figure 1.10 The schematic drawing shows domain organization in RePC where blue is BC, yellow is CT, red is BCCP, and green is allosteric domain (a). The schematic drawing shows the monomer A of RePC structure exhibiting each domain with the reaction catalyzed in the individual domain below (b) (19).

1.5 The quaternary structure of PC

The crystal structure of RePC tetramer co-crystalized with ethyl-CoA shows that PC is asymmetrical tetramer. RePC tetramer consists of two dimers interacting between interfaces of the neighbor BC and CT domains (Fig 1.10C). This tetramer contains two different faces. On each face, two monomers run antiparallel with each other, and they run in perpendicular with another face (Fig 1.10A). The crystal structure of RePC shows there are two acetyl-CoA binding sites per tetramer (19). The distance between BC and CT domains of the opposing polypeptide chain on one dimer pair where ethyl-CoA binds is approximately 65 Å (Fig 1.10B), whereas the distance between BC and CT of the another dimer pair is 80 Å (Fig 1.10C). Mutagenic and structural studies reveal that the BCCP domain swings between active-site pairs on opposing polypeptide chains rather than between active-site pairs of same polypeptide chains (Fig 1.10B). These structures suggest role of acetyl-CoA in relative orientation of individual domains. The acetyl-CoA binding with allosteric domain can activate catalysis by reducing the distance between neighboring active sites.

The study of St. Maurice et.al (19) exhibits the intermolecular catalysis of two opposing subunits by generating two RePC mutants in which each mutant harbors mutation in BC or CT domains. Each of these mutants shows zero activity however when these two mutants were combined to form the hybrid mutants, its enzymatic activity was regained to 50%, indicating that BC domain of one subunit and CT domain of opposing subunit of the same dimer pair forms intermolecular active site. Moreover, ethyl-CoA binding to each dimer pair changes position and orientation of BC domain of one dimer pair compared to the other (Fig 1.11). In dimers, superposition between monomer A, monomer that ethyl-CoA binds with, and monomer B, monomer that ethyl-CoA is unbound, shows an approximate 40˚ rotation and translocation of nearly 40 Å in the BC active site, centered at the ethyl-CoA binding site of the allosteric domain, whereas the CT domain shows the minor deviation (Fig 1.11). PC tetramer binding with acetyl-CoA causes rotation of BC domain on the top dimer that acetyl-CoA binds with. This reduced distance between active sites pairs of the top dimer to 65 Å, whereas the distance between active sites pairs of the bottom dimer where acetyl-CoA is unbound is 80 Å. The asymmetrical dimers between the top face where the active-site pairs are pushed closer than those of

the bottom face obstructs the acetyl-CoA binding on the bottom face and can describe half-site reactivity of PC.

The crystal structures of full-lenght PC from *Staphylococcus aureus* and C-terminal region of PC (missing only the BC domain) from human show difference in conformational state from the crystal structure of RePC (48). The tetramer of RePC is asymmetrical while the tetramer of SaPC is symmetrical (48). As shown in Fig.1.13, the carboxyltransferase and PC tetramerization (CT+PT) domain of HsPC and SaPC are in the same orientation. The PC tetramerization (PT) domain of SaPC and HsPC located at the central of the tetramer interface is involved in the tetramerization of the enzyme by mediating PT-PT contacts between subunits in different layers. However, the two PT domains in the bottom face of CT+PT domains from RePC are far from the two PT domains in the upper face indicating that the PT domain of RePC is not involved in the tetramerization of the enzyme (Fig. 1.13B) (48). Interestingly, the RePC monomer bound to ethyl-CoA is similar to the SaPC monomer without the activator (Fig. 1.13C) (48).

Though SaPC tetramer is symmetrical while RePC tetramer is asymmetrical, the recent study has shown the transformation from asymmetrical conformation to symmetrical conformation during the catalysis of SaPC (55). The study of cryoEM structure for SaPC obtained from a sample undergoing catalysis in the presence of all substrates shows mainly two types of conformations which are asymmetric and symmetric (55). In class 1, SaPC tetramer is asymmetrical conformation. The top layer of this class shows the position of BCCP domains in the active site of BC domain of its own monomer (Fig. 1.14A). The B-subdomain lid of the BC domain tilts and allows the BCCP domain entering into the BC active site (Fig 1.15B). The crystallopgraphic structure from RePC T882A can be fitted within the cryoEM map of the top layer of class 1 SaPC with the distance between the Lys residue where the biotin is attached and the BC active site is 19.7 Å (the average distance between two sites in the top layer of class 1 is 19.0 $\pm$ 1.8 Å) showing the similarity between this SaPC state and RePC (Fig. 1.16A and 1.16B**).** The bottom layer of class 1 shows the position of BCCP domains in an exo binding site located between its own BC domain and CT domain of an opposing monomer (Fig. 1.14B). The crystallographic structure of RePC can be fitted within the cryoEM map of the

bottom layer of class 1 SaPC, and the BCCP domain is also located in an exo binding site (Fig. 1.16C and 1.16D). These fits support that the structure of class 1 SaPC tetramer is asymmetrical conformation (55). In class 2, the BCCP domain of the top layer is in the active site of CT domain of the opposite monomer which supports to the previous study of the crystal structure of SaPC tetramer (Fig. 1.14C, 1.16E, and 1.16F). The class 2 of SaPC tetramer exhibits as the symmetrical conformation (55).

The structural data from cryoEM analysis reveals that the transformation between two conformations of SaPC is caused from the coupling between the structure and the position of the BCCP domain and the relative rotations between BC and CT domains and PT domains (55). In the top layer of class 1 SaPC which exhibits the asymmetrical conformation, the distance between BC active site of its own monomer and PT domain is closer than the distance between BC active site of the opposing monomer and PT domain which favors the BC reaction occurring within the same subunit (Fig. 1.17A). The tilted B-subdomain lid of BC domain only occurs in the top layer while this region in the bottom layer is closed which agrees with the negative cooperativity between layers of this enzyme (55). Then the BCCP domain moves approximately 65 Å to reach the CT active site of the opposing subunit by the support from the relative rotation between the BC and CT domains of its own monomer and the inward movement of the PT domains (Fig. 1.17B). Next, the PT domain shifts inward, and the BCCP domain moves to the exo binding causing the enzyme turn to the asymmetrical conformation (Fig. 1.17C). The enzyme finally returns to the symmetrical conformation again (Fig 1.17D). The position of PT domain of the asymmetrical conformation does not show the PT-PT contact, while the PT domain translocates into the central part in the symmetrical conformation allowing the presence of PT-PT interactions (55). The essential roles of the PT domain in the structural transformations of PC tetramers are to couple the relative changes between BC and CT domains, to alternate the inter- and intra-layer contacts between subunits, and to move the anchor points for the linker of the BCCP domain (55).

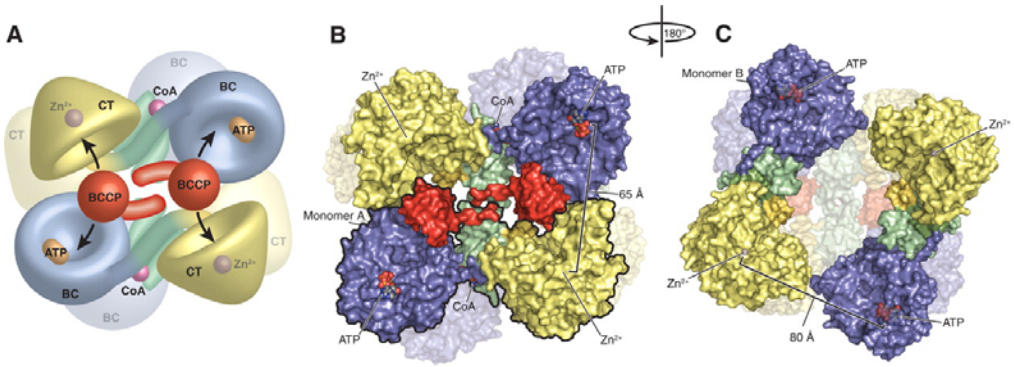

Fig 1.11 Model of RePC tetramer shows the movement of BCCP domain between two active sites of opposing polypeptidechains (A). The top surface of RePC where ethyl-CoA bound contains two monomers. One of them is outlined in black. The distance between the BC active site and CT active site of opposing monomer is 65 Å (B). The bottom surface of RePC where ethyl-CoA is unbound , the distance between BC active site and CT active site of opposing monomer is 80 Å (C) (19).

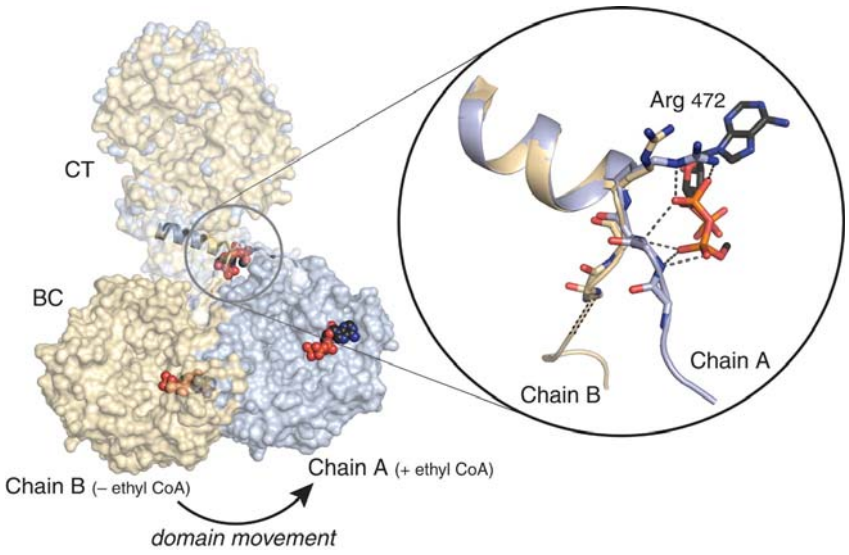

Fig 1.12 The position and orientation of BC domain is changed by the binding of ethyl-CoA. The allosteric domain of monomer A was aligned with the allosteric domain of monomer B. This superposition expresses minor deviation of CT domain, but significant deviation of BC domain can be observed. There are three residues of BC domain in monomer A, Arg^{472}, Gln^{470}, and Asp^{471}, that are deviated and form strong interaction with ethyl-CoA. However in monomer B where ethyl-CoA is unbound, Arg^{472} is projected away from the activator area. $Gln^{470}$and Asp^{471} are in different direction. (19).

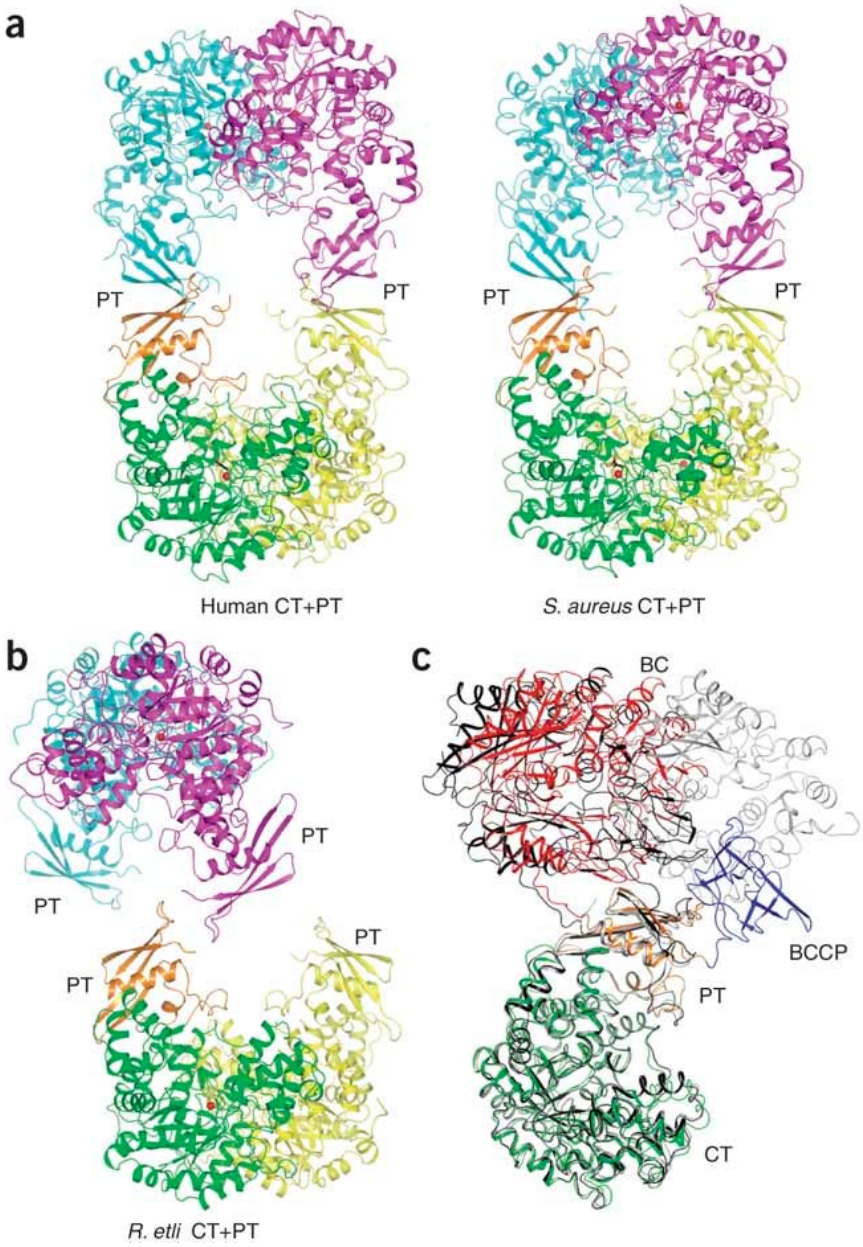

Fig 1.13 Different tetramer interface of HsPC and SaPC compared to that of RePC. The schematic drawings show the CT and PT (CT+PT) domain of HsPC and SaPC (A). The schematic drawing shows the CT+PT domain of RePC in the same orientation as in panel A (B). Overlay of the structure of monomer 1 in SaPC (colored), the monomer bound to ethyl-CoA of RePC (black), and the free monomer of RePC (C) (48).

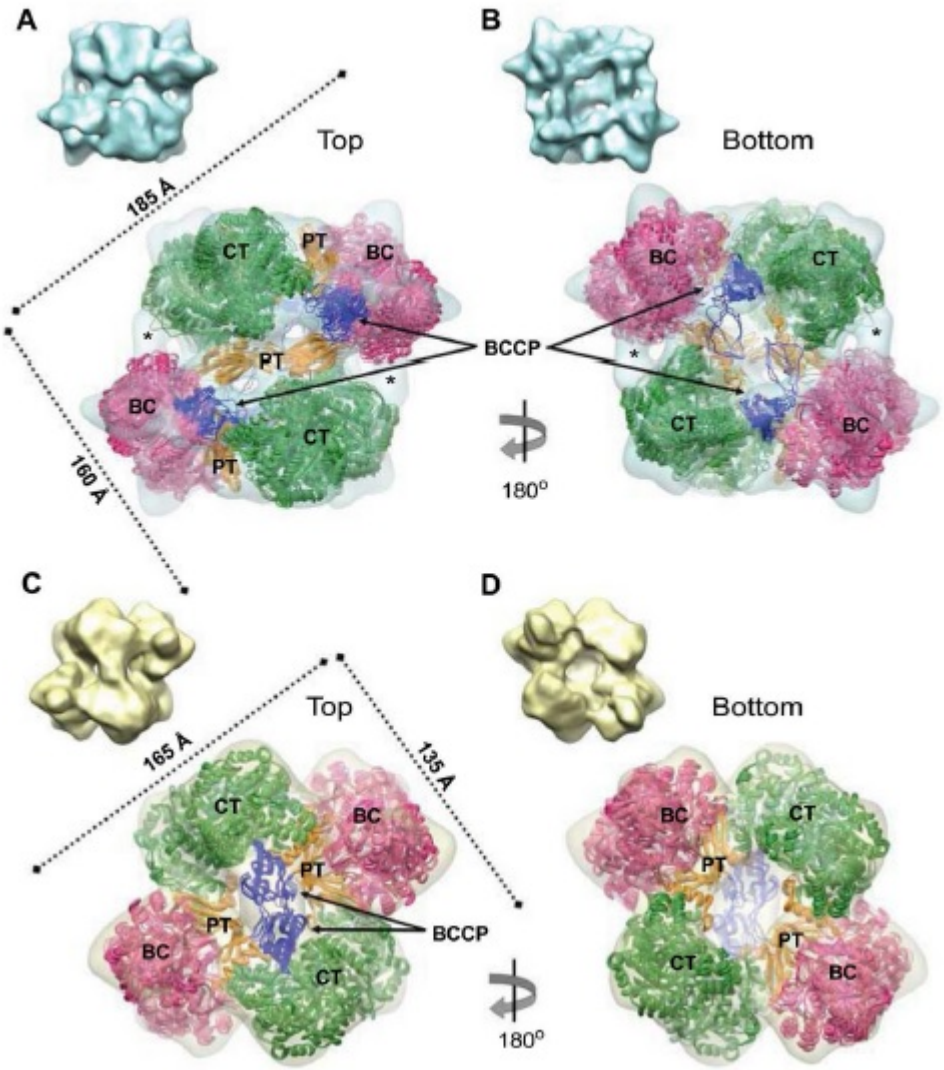

Fig 1.14 CryoEM maps for class 1 and class 2 conformers of SaPC tetramer. These maps are depicted in semi-transparent mode in order to visualize the atomic models generated for SaPC tetramers. There are five atomic models for each map as the results of five independent Molecular Dynamics Flexible Fittings (MDFF) runs. CryoEM maps exhibit the top layer of SaPC tetramer class 1 (A), the bottom layer of class 1 (B), the top layer of class 2 (C), and the bottom layer of class 2 (D) (55).

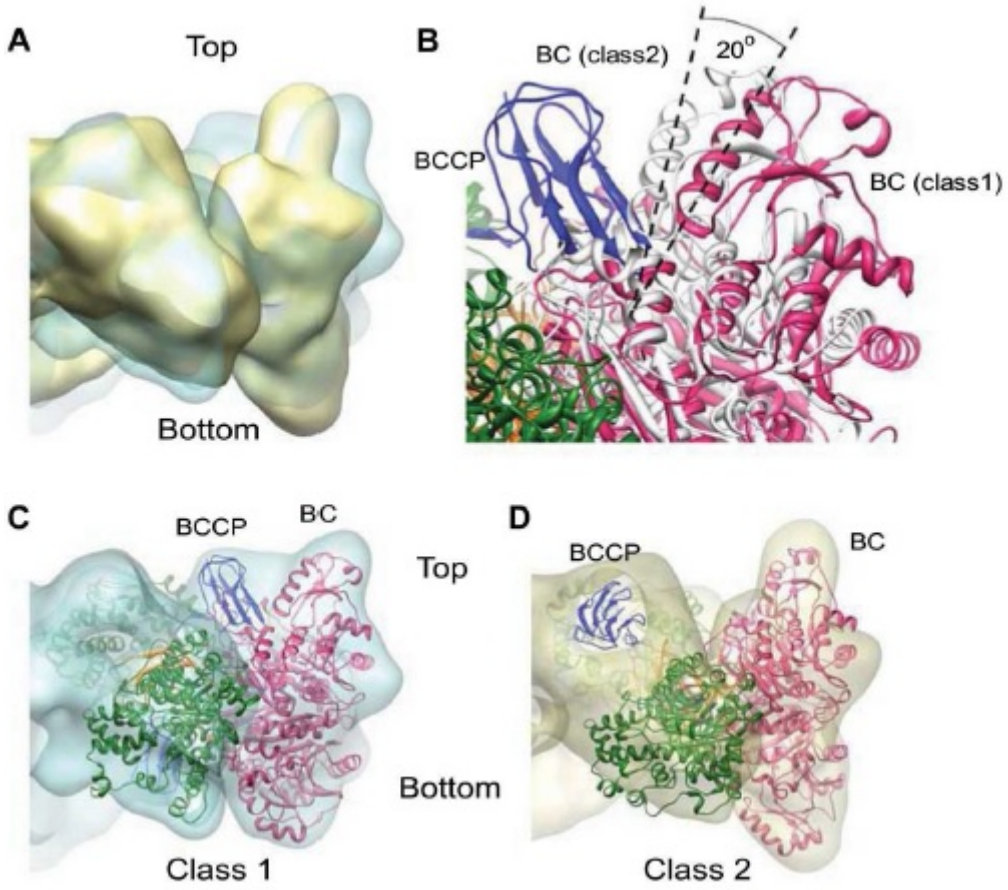

Fig 1.15 CryoEM maps show the different structures in the BC domains. The side view of BC regions from class 1 (blue) and class 2 (yellow) of SaPC tetramer in semi-transparent mode and solid mode respectively (A). The comparison between one of atomic models fitted in the class 1 map (colored) and one atomic model fitted in the class 2 map (grey) showing the tilted B-subdomain lid of BC domain between the atomic models (B). The fitting of one of atomic models with in the class 1 cryoEM map shows the fitted atomic model in semi-transparent mode (C). The fitting of one of atomic models with in the class 2 cryoEM map shows the fitted atomic model in semi-transparent mode and same orientation as in panel C (D) (55).

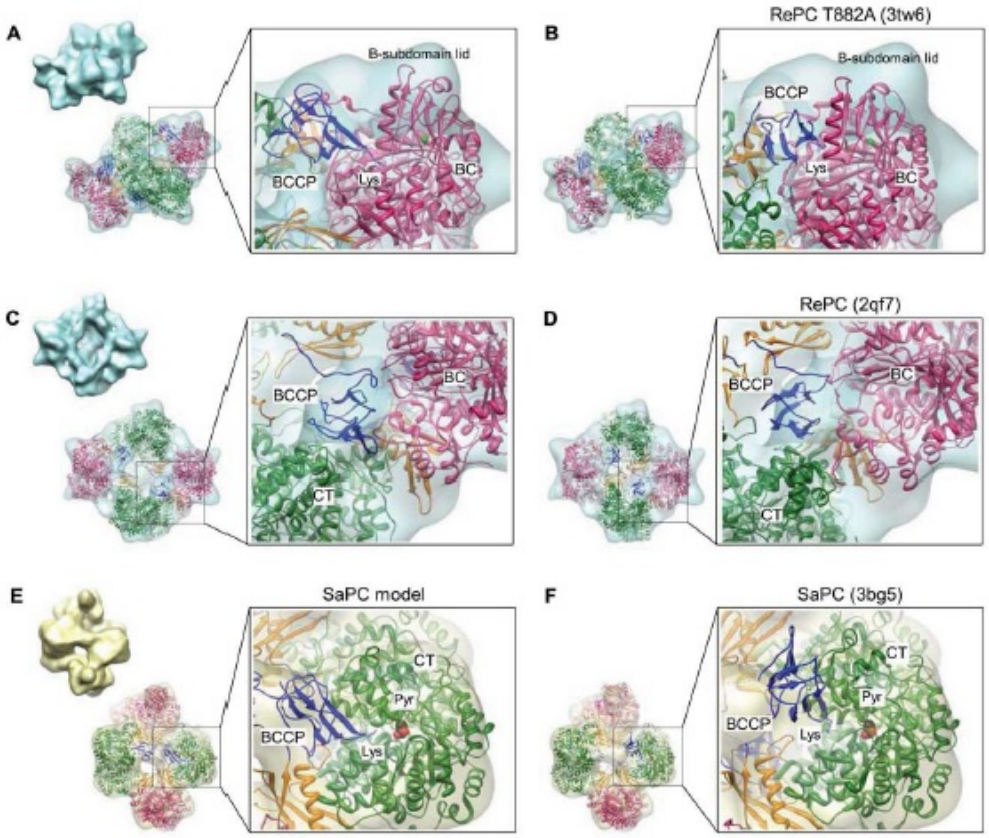

Fig 1.16 CryoEM maps of SaPC, RePC T882A, and RePC showing the position of BCCP domains. The semi-transparent cryoEM maps with ribbon models represent atomic data inside maps. The cryoEM maps of the top layer of SaPC tetramer class 1 show the BCCP domain bound to the BC domain of its own monomer. The average distance between the Lys where the biotin is attached and the BC active site of five models is 19.0 $\pm$ 1.8 Å (A). The fitting of crystallographic structure of RePC T882A mutant within the cryoEM map for SaPC tetramer class 1. The distance between the Lys residue and the BC active site is 19.7 Å (B). The cryoEM maps of the bottom layer of SaPC tetramer class 1 show the BCCP domain located in the exo binding site between BC and CT active sites (C). The fitting of crystallographic structure of RePC within the cryoEM map for SaPC tetramer class 1. The location of BCCP domain of this map is also in the exo binding site (D). The one of the atomic models from the MDFF for class 2 shows the position of BCCP near the CT active site of the opposite monomer. The average distance between the Lys and CT active site is 9.0 $\pm$ 1.3 Å (E). The fitting of crystallographic structure of SaPC within the cryoEM map for SaPC tetramer class 2. The distance between the Lys and CT active site is 9.4 Å (F) (55).

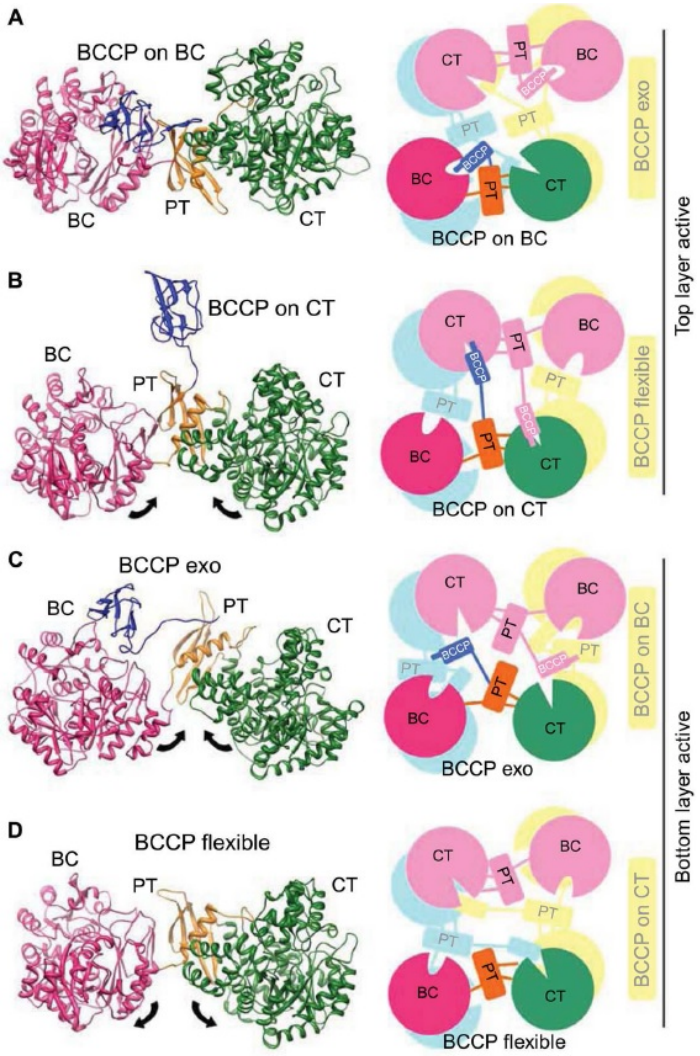

Fig 1.17 The atomaic models show four different structures of SaPC subunits. The ribbons represent the cryoEM maps of SaPC tetramer for top layer of class 1 (A), top layer of class 2 (B), bottom layer of class 1 (C), and bottom layer of class 2 (D), while the cartoon models on the right panels depict the architecture of the tetramers observed in class 1 (A), class 2 (B), class 1 upside-down (C), and class 2 upside-down (D) (55).

1.6 The allosteric regulation of PC by acetyl-CoA

The allosteric regulation is the process in which the enzyme is regulated by binding of an effector molecule at the specific site (known as the allosteric site). This allosteric site is located elsewhere and is not the active site of the enzyme. The regulation of enzyme can either activate or inhibit the enzyme activity. The α_4 PCs are allosterically activated by acetyl-CoA. Previous works have shown that the locus which acetyl-CoA stimulates PC activity is the biotin carboxylation reaction (32, 33, 34, 35, 36), not in the carboxyltransferase reaction (37). In chicken but not yeast PC (34), acetyl-CoA was able to increase the steady state rate of ATP phosphorylation (33, 34, 35) and the rate constant for the first order approach to steady state (35). Though pyruvate was absent, the rate constants for the approach to steady state of enzyme-carboxybiotin complex formation were raised by acetyl-CoA (34,35). In addition, acetyl-CoA reduces the affinity of nucleoside triphosphate binding in stopped-flow experiments with the fluorescent ATP analogue, formycin A 5-triphosphate (38). Study performed by Adina-Zada et al.(39) found that mutation of Lys1112 residue, covalently bound to biotin of *B. thermodentrificans*, was exploited in order to produce unbiotinylated apoenzyme, and the kinetic assay of carboxylation reaction to free biotin between the presence or absence of acetyl-CoA was compared. This study shows that in the presence of acetyl-CoA, the rate of reaction increased 8-fold higher than in the absence of acetyl-CoA. Therefore, it suggests that the rate of the carboxylation of biotin in overall reaction can be stimulated by acetyl-CoA.

A chimeric PC generated from the combination between the BC domain from acetyl-CoA independent PC (*A. aeolicus* PC) and the CT and BCCP domain from acetyl-CoA dependent PC (*B. thermodentrificans* PC) showed the activity that was independent from acetyl-CoA similar to whole *A. aeolicus* PC (40). The acetyl-CoA activation characteristics of 2 yeast isoenzymes of PC (Pyc1 and Pyc2) and chimeric constructs of these isoenzymes were investigated. Pyc1 and Pyc2 had different degrees of dependency on acetyl-CoA for the activities; they had different K_a for acetyl-CoA. In addition, they showed distinct degrees of co-operativity for the activation (9). Kondo *et al*. (41), two engineered forms of *B. thermodentrificans* PC, only the biotin carboxylase domain (BC form) and the carboxyltransferase with biotin carboxyl carrier protein (CT+BCCP form), were expressed and assayed. The BC form

retained the biotin-dependent ATPase activity, but this activity was not activated by acetyl-CoA with the free biotin as substrate. The CT+BCCP form had oxaloacetate decarboxylating activity but not stimulated by acetyl-CoA. Furthermore, the BC single protein from *B. thermodentrificans* PC exhibited ATPase activity when it was enhanced by acetyl-CoA in the presence of biotinylated BCCP as a substrate although lesser than in the intact enzyme (43). Therefore, it suggests that the acetyl-CoA binding site and its main locus of action are not completely located in the BC domain of PC. It may bind to other parts of enzyme (9).

The crystal structure of RePC bound to ethyl-CoA (19), a non-hydrolysable form of acetyl-CoA, showed the binding site of acetyl CoA locating between the BC and CT domains and between the CT and the BCCP domains. Most interestingly, there are only two ethyl-CoA binding sites per one tetramer. From St Maurice et al.(19), binding of ethyl-CoA affects the tetrameric conformation of PC by changing the position and orientation of BC domain to reduce distance between BC of one monomer and CT domain of another monomer in the same partner subunit. This inhibits acetyl-CoA binding at another face of PC tetramer, so it leads the biotin carboxylation and the carboxyl transfer occurring as half-site activity. There are many residues that might be important to acetyl-CoA binding. Arg427 and Arg472 are the two residues which directly interact with ethyl-CoA in the crystal structure. Mutations of these two residues to the R472S and R472K mutants markedly reduced acetyl-CoA dependent activity of the enzyme. The increase in K_m for MgATP and decrease in k_{cat}/K_m values in R472S and R472K mutations suggested the effect of these mutations on reaction steps from MgATP binding to the formation of carboxyphosphate (45). In addition R472S and R472K decreased the formation of carboxybiotin. The significant effects of R472 mutant on enzymatic activities were due to its strong disruption of interactions with 5'-α-phosphate of ethyl CoA (Fig 1.18) (45). However, R472S and R472K mutation did not affect the cooperative binding of acetyl-CoA. There might be interactions of acetyl-CoA with other residues crucial for the allosteric binding (45). From Figure 1.18, E1027appears to interact with R472 which binds to acetyl-CoA (45), so it is interesting to examine whether E1027 is relevant to acetyl-CoA activation. Other mutant in this study, increase in the catalytic rates of the acetyl-CoA-independent carboxylation of pyruvate or k^0_{cat} of R427S and R427K mutations

indicated the involvement of the interaction between R427 and adjacent residues in forcing the enzyme into less active structure (45). The schematic drawing shows the interaction between R427 and D1018 in the absence of acetyl-CoA (Fig 1.19), so it is interesting to investigate the role of D1018 on the activity of RePC. So based on the study of RePc crystal structure and the study of residues in allosteric domain (19, 45), D1018 and E1027, residues in the second part of allosteric domain which interact with R427 and R472, residues in the first part of allosteric domain, respectively were the target of this study.

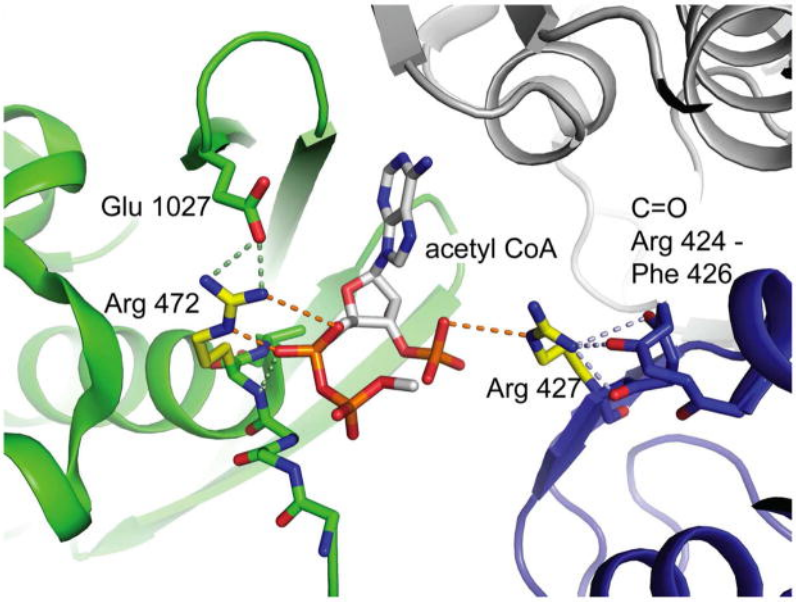

Figure 1.18 The interactions of Arg427 and Arg472 with ethyl-CoA, the acetyl-CoA analogue, and neighboring residues located in the acetyl-CoA binding site (45).

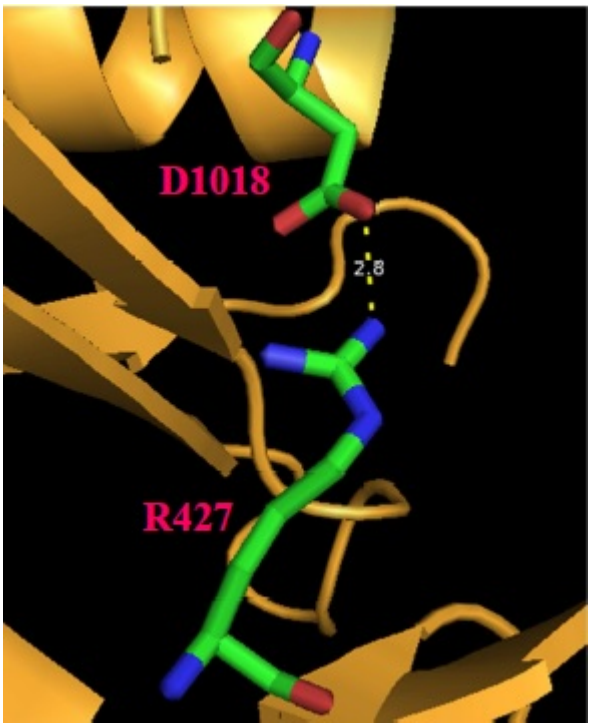

Figure 1.19 Schematic drawing show the interaction between R427 and D1018 in the absence of acetyl-CoA (This figure obtained from Pymol program).

Project rational

According to the crystal structure of RePC in complex with ethyl-CoA, it shows several residues relevant to allosteric binding and activation including R427 and R472. These two residues were examined, and results shown that there might be other residues relevant to acetyl-CoA stimulation. The schematic drawing shows the interaction between R427 and D1018 in the absence of acetyl-CoA while R472 interacts with E1027 in the absence and presence of acetyl-CoA. Therefore, the analysis of D1018 and E1027 was exhibited in order to probe their effect on the enzymatic activity activated by acetyl-CoA. The investigation was carried out by site-directed mutagenesis, and mutant enzymes were subjected to several enzymatic assays in order to understand more about the regulation of RePC by acetyl-CoA.

CHAPTER II
OBJECTIVES

1. To express wild-type and mutant *R. etli* pyruvate carboxylase in and *E. coli* expression system.

2. To study the effect of acetyl-CoA activation of D1018 mutants (D1018A, D1018N, and D1018R), E1027 mutants (E1027A, E1027Q, and E1027R), R469 mutants (R469S and R469K), and D471 mutant (D471A).

CHAPTER III
MATERIALS AND METHODS

3.1 Reagents

Ampicillin, chloramphenicol, bovine serum albumin (BSA), adenosine triphosphate (ATP), β-mercaptoethanol, phenylmethylsulfonylfluoride (PMSF), dithiothreitol (DTT), ethylenediaminetetra-acetic acid (EDTA), Tris-(hydroxymethyl)methylamine (Tris) and sodium dodecyl sulfate (SDS) were from Sigma.

Bacterial culture media; tryptone, yeast extract, bacto agar were purchased from Difco. Restriction endonuclease (*Sac*II and *Xho*I) and T4 DNA ligase were purchased from New England Biolabs. GeneJET Plasmid Miniprep Kit was obtained from Fermentas. NucleoSpin Plasmid Purification Kit and Nucleospin® DNA Extraction Kit were purchased from MACHEREY-NAGEL. Expression plasmid (pET-17b) was from Novagen and pBluescript II SK phagemid vector was from Stratagene. Oligonucleotide primers were synthesized by Bio Basic Inc. HisPur^{TM} Cobalt Resin was purchased from Pierce (Rockford, IL). Malate dehydrogenase (from pig heart), pyruvate kinase, lactate dehydrogenase (from hog muscle), glucose-6-phosphate dehydrogenase (from yeast grade I) and hexokinase (from yeast overproducer) were from Roche.

Acetyl-CoA was prepared as follows. Na_3CoA (25 mg/ml) and $KHCO_3$ (50 mg/ml) were dissolved in 8 ml distilled water on ice. 300 µl of acetic anhydride were added to the mixture prior to checking completion of reaction by spotting the solution on filter paper which had been soaked in 5,5'-dithiobis(2-nitrobenzoic acid) (DNTB) solution. If the reaction is not complete, the filter paper will turn yellow. The pH of the solution was then adjusted to 6.75 with 1 M NaOH. The concentration of acetyl-CoA was determined by enzymatic assay with citrate synthase and colormetric reaction with DTNB. The concentration of acetyl-CoA corresponding to that of DTNB was calculated using the extinction coefficient $\varepsilon 412 = 13.6\ mM^{-1}\ cm^{-1}$.

3.2 Construction of wild-type and mutant *Rhizobium etli* PC constructs

D1018A, D1018N, D1018R, E1027A, E1027Q, and E1027R were obtained from Associate Professor Sarawut Jitrapakdee.

R469S, R469K, and D471A were obtained from Mr.Chaiyos Sirithanakorn

3.3 Small-scale recombinant protein expression

The 500 µl starter cultures of *E. coli* BL21 harboring wild-type or mutant PC co-transformed with *E. coli* biotin protein ligase (*birA*) gene were inoculated in 50 ml LB broth containing 30 µg/ml chloramphenicol and 100 µg/ml ampicillin and cultured at 37ºC with shaking until their O.D. 600 reached 0.6-0.7. Then 5 ml of culture were induced without or with 1mM IPTG at 16ºC in shaking incubator overnight. 1 ml of sample was collected and analyzed on 7.5% reducing SDS-PAGE.

3.4 Analysis of protein solubility

500 ml culture of *E. coli* BL21 with bacterial biotin ligase (*birA*) gene and wild-type or mutant PC were induced with 1 mM IPTG and grown at 16ºC with vigorous shaking overnight. Then cell pellet was collected and resuspended in 5ml lysis buffer (50 mM NaH_2PO_4, 300 mM NaCl, 10 mM imidazole, pH to 8.0) containing 1 mg/ml lysozyme and incubated on ice for 30 min. Cells were sonicated with microtip for 3 min of 9 seconds pulse on and 9 seconds pulse off using a sonicator equipped with a microtip. Insoluble and soluble fractions were separated by centrifugation at 10,000 g for 30 min at 4ºC. Insoluble fraction was resuspended in 5 ml lysis buffer. Bradford's method was obtained to measure the protein concentration of each fraction. Various known concentrations of BSA (Protein standard II, Bio-rad) were diluted with distilled water and mixed with 200 µl of 1/5 diluted dye reagent. The mixtures were incubated at room temperature for at least 5 min before measuring an absorbance at 595 nm using microplate reader (Thermo Labsystem). The concentration were diluted with distilled water and mixed with 200 µl of 1/5 diluted dye reagent.

The mixtures were incubated at room temperature for at least 5 min before measuring an absorbance at 595 nm using microplate reader (Thermo Labsystem). The concentration of protein standard in the sample was calculated by referring to the concentrations of protein standard. 20 μg protein of each fraction were used for SDS-PAGE analysis.

3.5 Purification of PC by cobalt column chromatography

500 ml-overnight culture of *E. coli* BL21 habouring biotin ligase (*birA*) gene and wild-type or mutant PC was sub-cultured into 8 L of LB-broth supplemented with 6.25 g/L arabinose, 0.2 g/L ampicillin, 30 mg/L chloramphenicol, 10 mg/L biotin, and 2 ml antifoam. The culture was grown with shaking at 37°C until OD_{600} of the culture reached 1.0. Then the culture was induced with 0.1 mM IPTG with shaking at 16ºC for 36 h. Bacterial cells were harvested by centrifugation at 5,000g and washed with 100 mM Tris-HCl and 1 mM EDTA pH 7. Then cell pellet was suspended in loading buffer (50 mM NaH_2PO_4, 300 mM NaCl, 10 mM imidazole, pH 7.4) containing 1 mg/ml lysozyme for 30 min before mechanical disruption cells by a Bead-Beater™. The soluble fraction was collected by centrifugation at 12,000 rpm for 25 min at 4ºC to remove cell debris. 1 ml of this fraction was collected for SDS-PAGE analysis while the remaining was mixed with 0.035 % (w/v) protamine sulfate to remove nucleic acid and centrifuged at 14,000 rpm for 30 min at 4 ºC. Then protein precipitation was performed by using 36 % (w/v) saturated ammonium sulfate and centrifuged at 14,000 rpm for 30 min at 4 ºC. The pellet was resuspened in 10 ml loading buffer before adding 40 ml Talon™ cobalt resin column. The column was washed 3 times with loading buffer and eluted with 40 ml elution buffer (50 mM NaH_2PO_4, 300 mM NaCl, 150 mM imidazole, pH 7.4). PC was partially purified by precipitating with 36 % (w/v) saturated ammonium sulfate and centrifuged at 14,000 rpm for 30 min at 4 ºC. The purified enzyme was resuspended and stored at -80 ºC in storage buffer (30% (v/v) glycerol, 100 mM Tris-HCl, pH7.8, and 1 mM DTE).

3.6 Spectrophotometric assay for quantitation of biotin in RePC

Because only fully biotinylated RePC can function, all wild-type and mutant were subject to the biotin quantitation before . This assay detects the binding of biotin to avidin. In order to be detectable by visible spectrophotometry, HABA dye or 2-(4'-hydroxyazobenzene) benzoic acid was performed to determine the biotinylation. The experiment contains two steps. The first step, enzyme digestion, the enzyme was incubated with 0.2% chymotrypsin and 0.1% pronase in a total volume of 100 µl at room temperature overnight. The second step was performed by preparing various biotin concentrations for standard curve. Then the mixture was incubated at 90-100 ˚C for 10 minutes in order to get rid of protease and measured with 0.5 mg/ml avidin and 10 mM HABA. The spectrophotometer was set at zero by using an empty cuvette. All samples and standards were measured absorbance at 500 nm. All samples were compared with the biotin standard curve.

3.7Enzyme assay

Effects of mutations at allosteric site in RePC were investigated by performing couple enzymatic reactions which are pyruvate carboxylation and ATP cleavage (Table 3.1). All assays were performed at 30 ˚C in a total volume of 1 ml. Data were collected in triplicate using a spectrophotometer interfaced to a PC equipped with a data acquisition program.

Table 3.1 Enzymatic reactions and coupled enzymes used for investigating the effects of mutation of RePC on their enzymatic activities. The highlighted products in boxes are assayed to examine the specific activities and initial rates.

Reactions	Couple enzymes
Pyruvate carboxylation The overall reaction catazyed in BC and CT active sites (forward) $MgATP + HCO_3^- + \text{pyruvate} \xrightleftharpoons{\text{Acetyl-CoA, } Mg^{2+}} \text{oxaloacetate} + MgADP + P_i$	**malate dehydrogenase** $\text{oxaloacetate} + NADH \rightleftharpoons \text{malate} + NAD^+$
ATP cleavage The first partial reaction catalyzed in BC active site (forward) $MgATP \xrightleftharpoons{\text{Acetyl-CoA, } Mg^{2+}, HCO_3^-} MgADP + P_i$	**pyruvate kinase** $\text{phosphoenol pyruvate} + ADP \rightleftharpoons \text{pyruvate} + ATP$ **lactate dehydrogenase** $\text{pyruvate} + NADH \rightleftharpoons \text{lactate} + NAD^+$

3.7.1 Assays of pyruvate carboxylation activity

The activity of wild-type and mutant RePC is measured in duplicate using a coupled spectrophotometric assay in which the oxaloacetate was converted to malate by malate dehydrogenase. The oxidation rate of NADH in this coupling reaction can be monitored by measuring the decrease of absorbance at 340 nm .

To determine the acetyl-CoA independent dependent (0.25 mM of acetyl-CoA) activity of mutant RePCs compared with wild-type, 30 µg protein of wild-type or mutants were used in 1 ml reaction mixture containing 100 mM Tris-HCl (pH 7.8), 2.5 mM ATP, 8 mM $MgCl_2$, 10 mM NaHCO3, 10 mM pyruvate, 0.1 mM NADH and malate dehydrogenase (5 U) and performed at 30ºC.

The K_a acetyl-CoA was determined by varying concentrations of acetyl-CoA at fixed concentrations of other reaction components. The k_{cat} value was calculated by dividing initial velocity by the enzymic biotin concentration in each assay.

3.7.2 ATP-cleavage assay

This reaction represents the first partial reaction catalyzed in BC active site (forward). The assay was conducted by coupling with the reactions catalyzed by pyruvate kinase and lactate dehydrogenase in 1 ml reaction mixture containing 20 µM of PC, 0.1 M Tris-HCl pH 7.8, 20 mM $NaHCO_3$, 1 mM ATP, 8 mM phosphoenol pyruvate, 5 mM $MgCl_2$, 0.22 mM NADH, 10 mM phosphoenolpyruvate, 5 units of pyruvate kinase, and 4 units of lactate dehydrogenase in the presence or absence of 5 mM acetyl-CoA at 30°C. The k_{cat} value was calculated by dividing initial velocity by the enzymic biotin concentration in each assay.

3.8 Data analysis

All data obtained from pyruvate carboxylation assay were analyzed by non-linear least square regression fit of the data to Hill equation (1). From equation (1), A is acetyl-CoA concentration, K_a is the activation constant, and the apparent k_{cat} is the apparent first order rate constant at each concentration of acetyl CoA, k^0_{cat} is the apparent first order rate constant at zero acetyl-CoA, h is the Hill coefficients and k_{cat} is the maximum calculated apparent first order rate constant.

$$k_{cat}^{app} = k_{cat}^{0} + \frac{k_{cat} \cdot [A]^h}{K_a^h + [A]^h} \quad (1)$$

CHAPTER IV
RESULTS

4.1 Small-scale recombinant protein expression

The N-terminal hexahistidine tagged wild-type and mutant RePC were expressed in *E. coli* BL21 (DE3). Their cultures were induced with or without 1 mM IPTG at 25 ˚C with shaking for 5 h. Whole cell lysates of non-induced and induced cultures were analyzed by 7.5% denaturing SDS-PAGE and stained with Comassie blue. Results in Fig. 4.1 and 4.2 showed that all mutants expressed a predominant band at approximate molecular weight of 130 kDa which corresponds to the molecular weight of monomer of RePC.

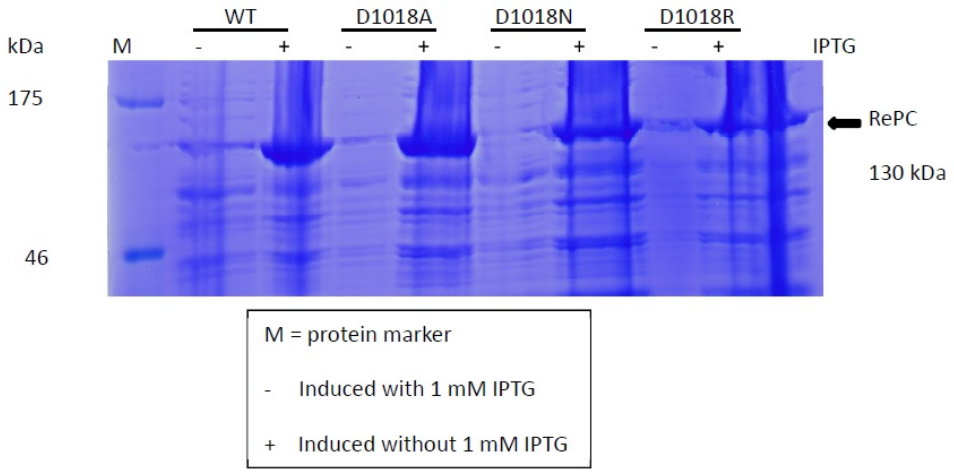

Figure 4.1 Whole cell extracts of D1018A, D1018N, and D1018R induced with or without IPTG were analyzed by SDS-PAGE analysis. The protein bands were stained with Coomassie blue R250.

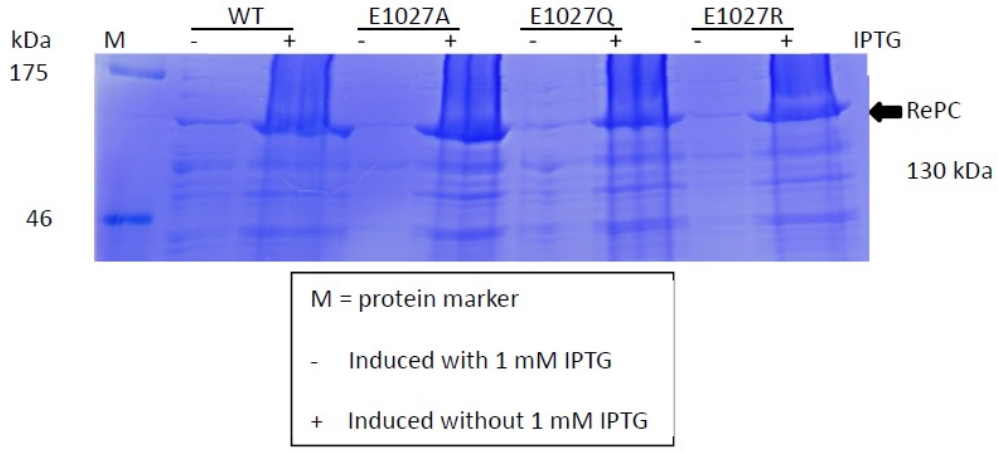

Figure 4.2 Whole cell extracts of E1027A, E1027Q, and E1027R induced with or without IPTG were analyzed by SDS-PAGE analysis. The protein bands were stained with Coomassie blue R250.

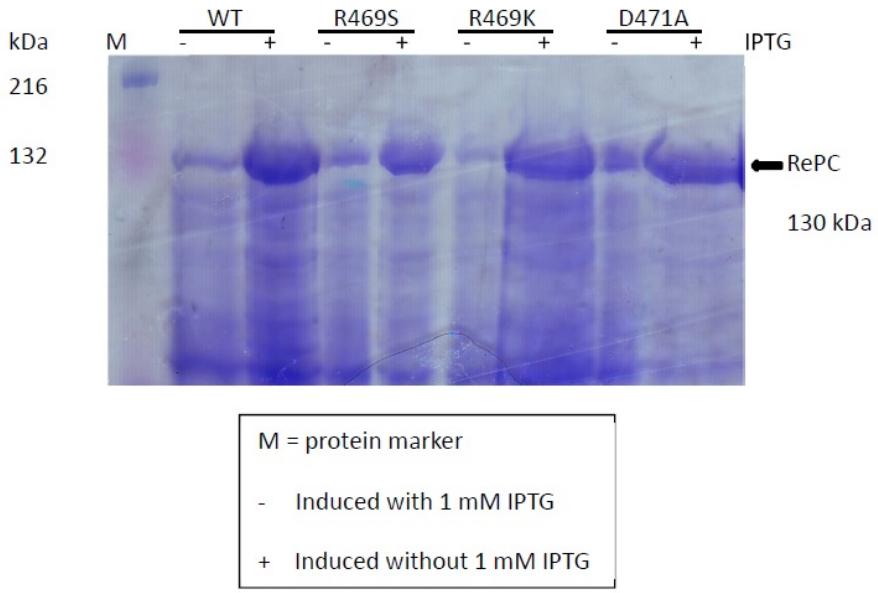

Figure 4.3 Whole cell extracts of R469S, R469K, and D471A induced with or without IPTG were analyzed by SDS-PAGE analysis. The protein bands were stained with Coomassie blue R250.

4.2 Analysis of protein solubility

Inclusion body is the aggregated material which is normally found when recombinant protein is overexpressed in *E. coli*. This analysis was performed to compare the ratio of inclusion body and the soluble material of all mutant expression. The process began by growing wild-type and mutant RePC in *E. coli* at 37˚C before inducing with IPTG at 16 ˚C overnight (45). After cell disruption, soluble and insoluble proteins were separated by centrifugation. Supernatant and pellet were analyzed by SDS-PAGE. As shown in Fig. 4.4, 4.5, and 4.6, more than 50% of wild-type and all mutant RePC were found in soluble fraction.

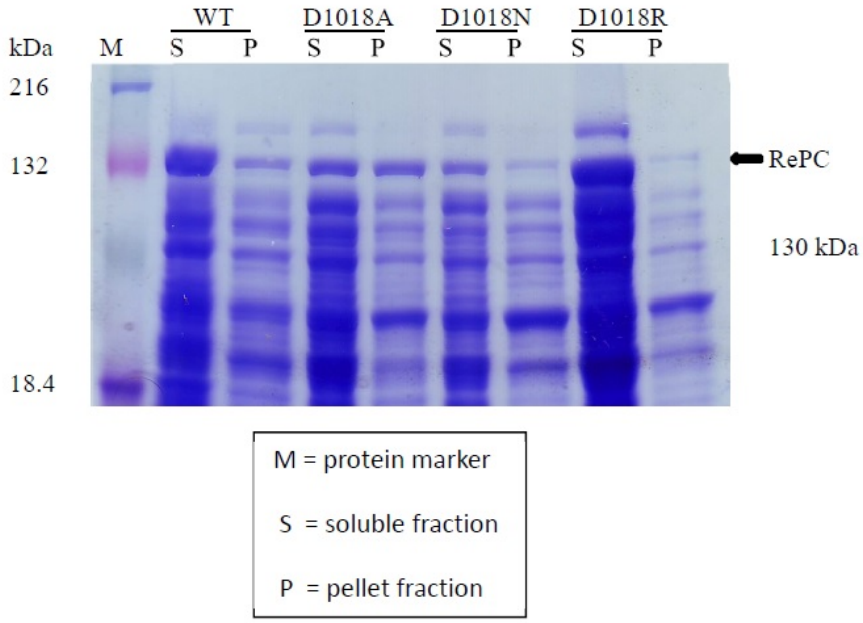

Figure 4.4 SDS-PAGE analysis of WT, D1018A, D1018N, and D1018R presence in soluble and insoluble (pellet) fractions.

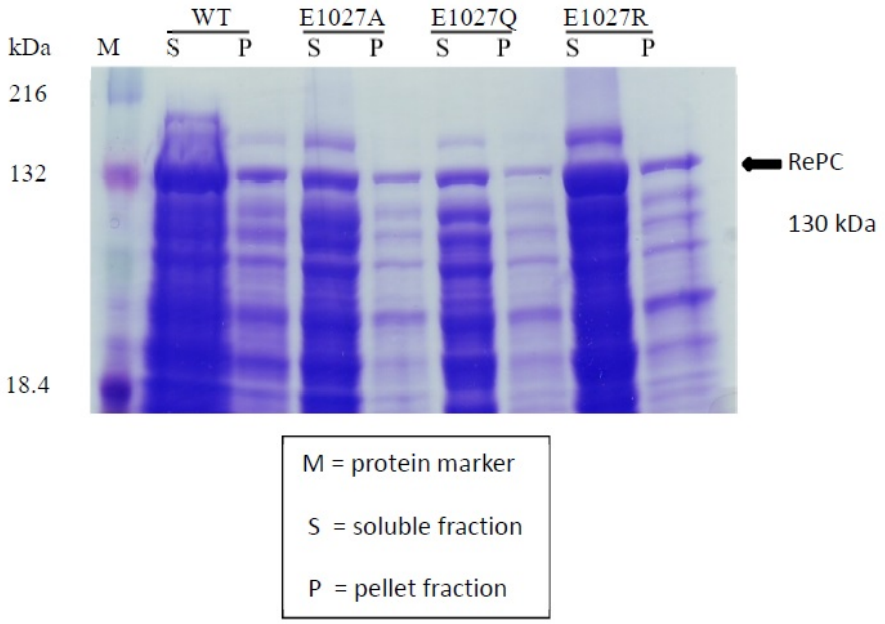

Figure 4.5 SDS-PAGE analysis of WT, E1027A, E1027Q, and E1027R presence in soluble and insoluble (pellet) fractions.

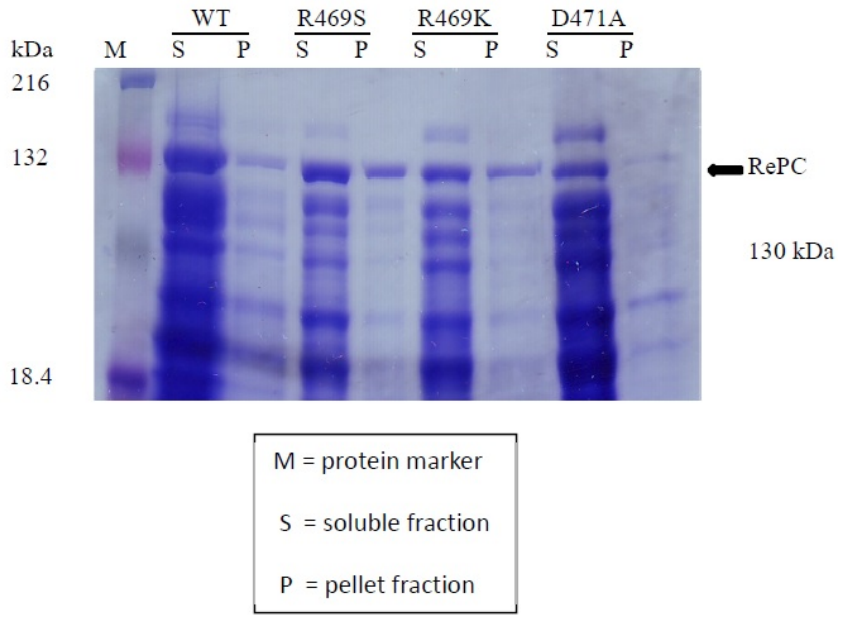

Figure 4.6 SDS-PAGE analysis of WT, R469S, R469K, and D471A presence in soluble and insoluble (pellet) fractions.

4.3 Large-scale recombinant protein expression and purification

The soluble fraction of hexahistidine tagged RePC was purified by ammonium sulphate precipitation followed by cobalt column chromatography. The average yield of mutant RePC from large-scale expression was 4-5 mg/L. The purity of enzyme was determined by SDS-PAGE analysis as shown in Fig 4.7 and 4.8

.

Figure 4.7 SDS-PAGE analysis for wild-type (WT), D1018A, D1018N, D1018R, E1027A, E1027Q, and E1027R mutant RePC purified by two step using ammonium sulphate precipitation followed by cobalt column chromatography.

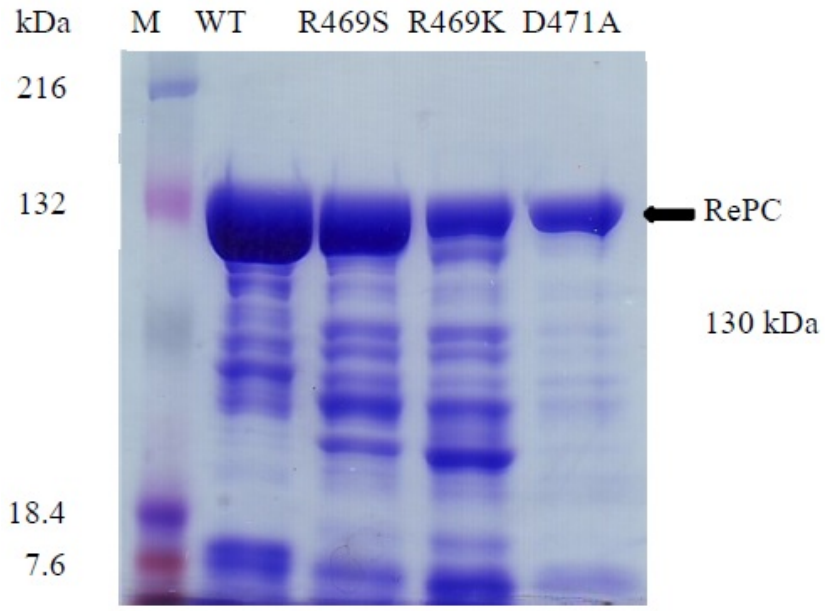

Figure 4.8 SDS-PAGE analysis for wild-type, R469S, R469K and D471A mutant RePC purified by two step using ammonium sulphate precipitation followed by cobalt column chromatography.

4.4 Biotin assay

The absorbance of wild-type and all mutant RePC were compared with the biotin standard curve and transfer as concentration. Then their concentrations were calculated equivalent to 1 mg protein as μmol. All results were shown in Table 4.1.

Table 4.1 Results from biotin assay of wild-type and all mutant RePC.

Enzyme	biotin concentration in prep enzyme (µmol/ml)
Wild-type	0.035
D1018A	0.01
D1018N	0.021
D1018R	0.018
E1027A	0.013
E1027Q	0.017
E1027R	0.015
R469S	0.017
R469K	0.017
D471A	0.139

4.5 Pyruvate carboxylase activity

The pyruvate carboxylation assay was performed to observe effects of mutations on the overall enzymatic reaction compared with wild-type enzyme. As shown in Table 4.2. The apparent k_{cat} for wild-type RePC was 18.408 $\pm$ 0.375 s^{-1}while that of D1018N and D1018 R was 56% and 30% of the wild-type enzyme respectively. However the k_{cat} of D1018A was 37% increase compared to the wild-type RePC. For E1027 mutations, the k_{cat} of E1027A and E1027Q was 39% and 57% increase from the wild-type RePC, while that of E1027R was only 19% of the wild-type enzyme. For R469 mutations, the k_{cat} of R469S and R469K was 60% and 31% of that of wild-type RePC. However, the pyruvation carboxylation activity of D471A was completely abolished as no detectable pyruvate carboxylation activity at saturated concentration of acetyl-CoA.

To determine if mutations affect acetyl-CoA dependent activity, D1018A and D1018R mutants were further investigated by performing pyruvate carboxylation assays at fixed concentration of substrates but varying the concentrations of acetyl-coA. As shown in Fig. 4.9, with solid lines representing fits of data to equation (1) and kinetic parameters derived from these fits are shown in Table 4.3, the apparent k_{cat} , K_a, and Hill coefficients or cooperativity parameter (h) for D1018A and D1018R were slightly changed. However, the apparent catalytic rate constants in the absence of acetyl-CoA or k^0_{cat} for D1018A and D1018R were 12- and 8 fold, higher than that of wild-type RePC, respectively.

The same assay was performed with E1027A and E1027R mutants and shown in Fig 4.10, with solid lines representing fits of data to equation (1) and kinetic parameters derived from these fits are shown in Table 4.4. The apparent k_{cat} , the apparent catalytic rate constants in the absence of acetyl-CoA or k^0_{cat} , and Hill coefficient or cooperativity parameter (h) of E1027A were slightly changed, but the apparent catalytic rate constant in the absence of acetyl-CoA or k^0_{cat} for E1027A was about 22-fold higher than that of wild-type RePC. For E1027R, the apparent catalytic rate constant in the absence of acetyl-CoA or k^0_{cat} and Hill coefficient or cooperativity parameter (h) for E1027R were also slightly changed from that of wild-type RePC. Interestingly, there was a decrease in the apparent k_{cat} for E1027R which was only16% of the wild-type enzyme. Moreover, activation constant or K_a of acetyl-CoA for

E1027R was 10 fold higher than that of wild-type RePC.

The pyruvate carboxylation activities of R469S and R469K were also performed at fixed concentration of substrates while acetyl-CoA concentrations were varied. As shown in Fig 4.11, solid lines represents fits of data to equation (1), and kinetic parameters derived from these fits are shown in Table 4.5. The apparent catalytic rate constants in the absence of acetyl-CoA or k^0_{cat}, the apparent k_{cat}, K_a, and Hill coefficients or cooperativity parameter (h) for R469S were slightly changed from that of the wild-type RePC. For R469K, the k^0_{cat} and K_a of acetyl-CoA for R469K were 4- and 5- fold higher than that of wild-type enzyme respectively. The apparent k_{cat} for R469K was 37% of that of wild-type RePC. Interestingly, R469K caused a drastic change in Hill coefficients or cooperativity parameter (h) which is 0.9 compared with wild-type RePC.

Table 4.2 Pyruvate carboxylation of wild-type, D1018A, D1018N, D1018R, E1027A, E1027Q, E1027R, R469S, R46K, and D471A RePC. All substrates' concentrations were fixed, and acetyl-CoA concentration was 0.25 mM.

Enzyme	k_{cat} (sec^{-1})	
	Without acetyl-CoA	With acetyl-CoA
Wild-type	0.182 ± 0.007	18.408 ± 0.375
D1018A	1.911 ± 0.097	25.123 ± 1.946
D1018N	0.549 ± 0.045	5.568 ± 1.127
D1018R	1.458 ± 0.034	10.301 ± 0.626
E1027A	4.118 ± 0.298	25.527 ± 3.04
E1027Q	3.239 ± 0.857	28.857 ± 1.519
E1027R	0.863 ± 0.125	3.481 ± 0.172
R469S	1.405 ± 0.059	11.069 ± 0.127
R469K	0.554 ± 0.079	5.618 ± 0.128
D471A	0.105 ± 0.004	0.105 ± 0.001

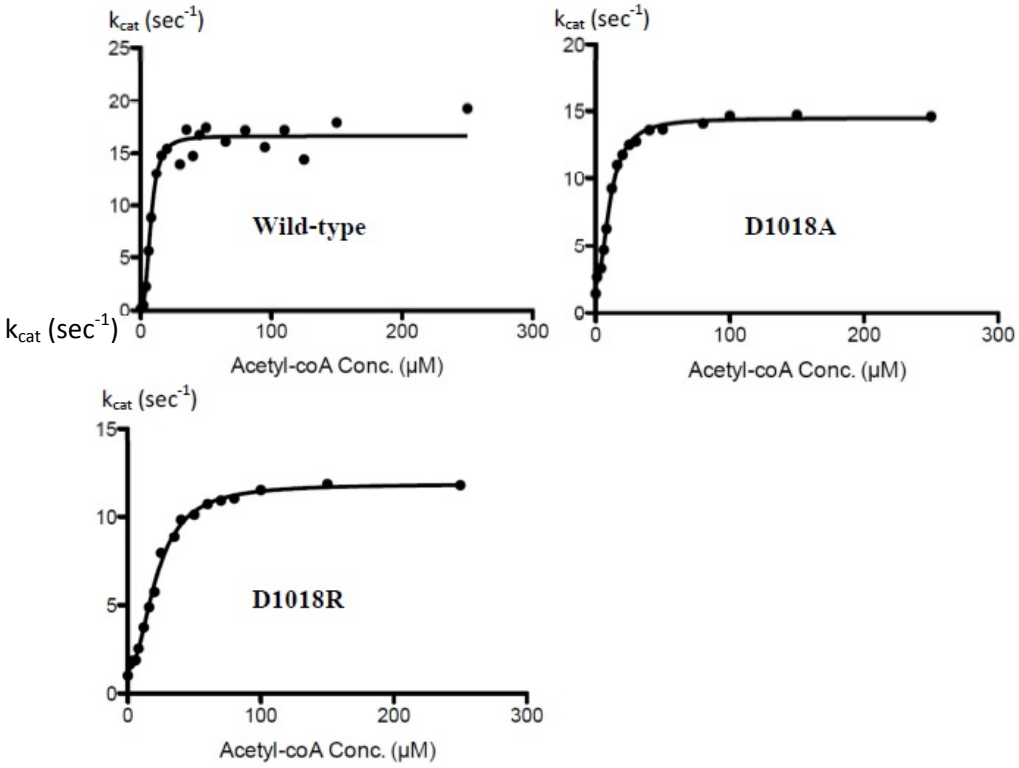

Figure 4.9 Effect of acetyl-CoA variation on the pyruvate carboxylation rate of wild-type and D1018 mutant RePC at fixed concentration of other substrates.

Table 4.3 Kinetic parameters for the pyruvate carboxylation reaction catalyzed by wild-type RePC and D1018 mutants. This reaction was fixed substrates' concentrations while acetyl-CoA concentration was varied. These parameters were obtained by fits of the data to equation (1).

Enzyme	Wild-type	D1018A	D1018R
k^0_{cat}	0.18 ± 0.01	2.17 ± 0.25	1.35 ± 0.16
k_{cat} (sec^{-1})	16.51 ± 0.76	12.32 ± 0.35	10.5 ± 0.26
K_a (µM)	7.73 ± 0.6	10.86 ± 0.49	21.68 ± 0.72
h (cooperativity parameter)	2.66 ± 0.48	2.06 ± 0.16	2.1 ± 0.14

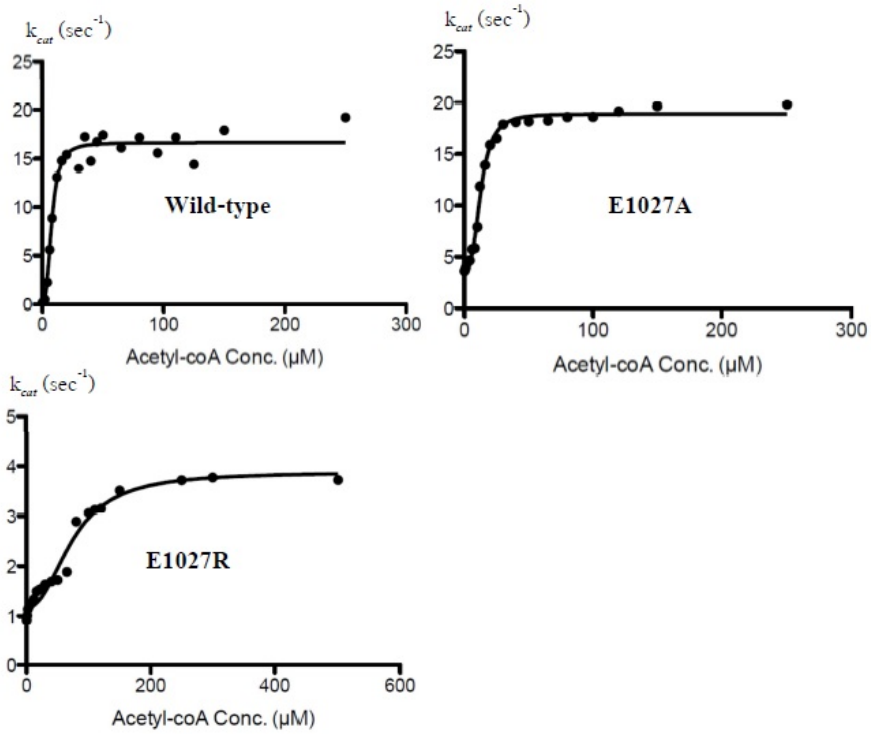

Figure 4.10 Effect of acetyl-CoA concentration on the pyruvate carboxylation rate of wild-type and E1027 mutant RePC at fixed concentration of other substrates.

Table 4.4 Effects of E1027 mutations on acetyl-CoA activation of pyruvate carboxylation.

Enzyme	Wild-type	E1027A	E1027R
k^0_{cat}	0.18 ± 0.01	3.94 ± 0.28	1.18 ± 0.07
k_{cat} (sec^{-1})	16.51 ± 0.76	14.93 ± 0.38	2.71 ± 0.18
K_a (μM)	7.73 ± 0.6	12.85 ± 0.45	74.82 ± 6.36
h (cooperativity parameter)	2.66 ± 0.48	3.04 ± 0.28	2.25 ± 0.37

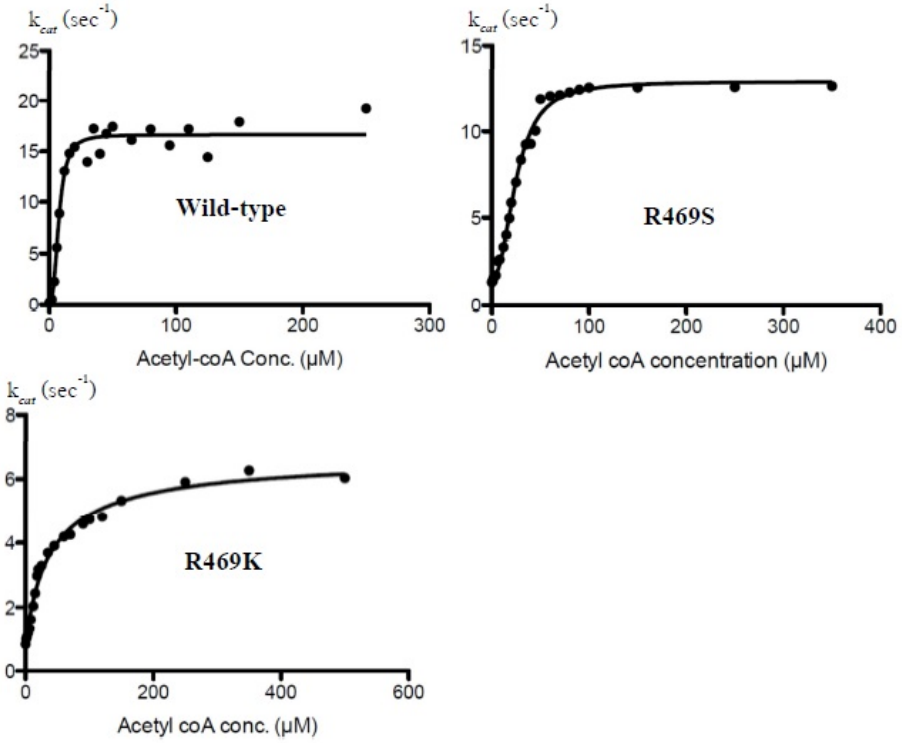

Figure 4.11 Effect of acetyl-coA concentration on the pyruvate carboxylation rate of wild-type and R469S and R469K RePC at fixed concentration of other substrates

Table 4.5 Kinetic parameters for the pyruvate carboxylation reaction catalyzed by wild-type RePC and R469 mutants. This reaction was fixed substrates' concentrations while acetyl-CoA concentration was varied. These parameters were obtained by fits of the data to equation (1).

Enzyme	Wild-type	R469S	R469K
k^0_{cat}	0.18 ± 0.01	1.61 ± 0.15	0.68 ± 0.16
Apparent k_{cat} (sec^{-1})	16.51 ± 0.76	11.28 ± 0.26	6.05 ± 0.44
K_a (μM)	7.73 ± 0.6	25.44 ± 0.79	39.9 ± 5.98
h (cooperativity parameter)	2.66 ± 0.48	2.34 ± 0.15	0.9 ± 0.1

4.6 ATP-cleavage reaction

Because the locus of action of acetyl-CoA is resided in the BC domain where ATP-cleavage reaction occurs (32, 33, 34, 35, 36), this activity in all mutants was investigated further. As shown in Table 4.9, the ATP cleavage activity of wild-type RePC in the presence of acetyl-CoA was 0.529 $\pm$ 0.006 sec^{-1} while those of D1018A and D1018R were 8- and 6- fold increased from wild-type. For E1027 mutations, E1027A showed 8- fold increase in activity while E1027R had approximately 3- fold increase compared with the wild-type. In R469 mutants, the ATP cleavage activity of R469S and R469K was 7- and 5- fold increase from the wild-type respectively.

The ATP cleavage activity in the absence of acetyl-CoA of wild-type RePC was 0.058 $\pm$ 0.002 sec^{-1}while those of D1018A and D1018R were increased approximately 35- and 25- fold higher than the wild-type. E1027A and E1027R had ATP cleavage activity 56- and 7- fold higher than the wild-type. R469S and R469K also had the activity 34- and 23- fold higher than the wild-type.

Table 4.6 The ATP-cleavage activity of wild-type RePC, D1018A, D1018R, E1027A, E1027R, R469S, and R469K mutants in the absence and presence of saturated concentrations of acetyl-CoA.

Enzyme	Activity without acetyl-CoA (s^{-1})	Activity with acetyl-CoA (s^{-1})
Wild-type	0.058 ± 0.002	0.529 ± 0.006
D1018A	2.05 ± 0.002	4.382 ± 0.088
D1018R	1.455 ± 0.137	2.969 ± 0.059
E1027A	3.248 ± 0.128	4.1 ± 0.032
E1027R	0.388 ± 0.035	1.493 ± 0.031
R469S	1.978 ± 0.044	3.746 ± 0.148
R469K	1.33 ± 0.079	2.821 ± 0.025

CHAPTER V
DISCUSSION

The recent identification of the allosteric domain in the crystal structure of RePC in complex with ethyl-CoA , an acetyl-CoA analogue has highlighted several residues which interact with this allosteric molecule (19). Two of them are R427 and R472 residues which are located in the first part of the allosteric domain. Site-directed mutagenesis of R427 and R472 and enzymatic activity of the resulting mutants were performed. These studies showed that mutations of the above residues appear to affect the biotin carboxylase activity of the enzyme. Due to remote distance between these two residues and the BC domain active site, the positioning and orientation of the BCCP domain and the binding of biotin at the BC active site influenced by the association between R427 and R472 with other molecules was proposed (45). The interaction of R427 with other residues in the absence of acetyl-CoA was speculated since the increase in the catalytic rates of the acetyl-CoA-independent pyruvate carboxylating activity or k^0_{cat} was observed in R427 mutant. Re-examination of the crystal structure of RePC has shown that D1018 appears to contact with R427 only in the absence of acetyl-CoA. Mutation of D1018 to alanine (D1018A) was performed in order to observe whether size and polarity constribute to this interaction. Mutation of this residue to asparagine (D1018N) was also investigated in order to observe whether the carboxylic acid side chain (negative charge) of aspartate residue contributes to this interaction. Lastly, mutation of D1018 to arginine (D1018R) was investigated to examine whether introducing reverse charge (positively charge of arginine) side chain would disrupt such interaction.

With respect to the second residue, viz., R472 was previously shown to interact with ethyl-CoA. Since both R472S and R472K showed an increased K_a for acetyl-CoA, this result suggests that mutation reduces the binding affinity of enzyme to acetyl-CoA. Moreover, decreased k_{cat}/K_m for R472S and R472K mutants indicated the greater impact on reaction steps from MgATP binding to the biotin carboxylation

than effects from R427S and R427K did (45). Furthermore, R472 mutations did not affect the cooperative binding of acetyl-CoA further suggests the presence of other residues which may also interact with this allosteric activator (45). Re-examination of RePC structure reveals that E1027 which is located in the second part of the allosteric domain appears to contact with R472 both in the absence and presence of acetyl-CoA. Mutation of E1027 to alanine (E1027A) was performed in order to examine the roles of size and polarity of this residue. Mutation of this residue to glutamine (E1027Q) was also studied because glutamine has polar uncharged side chain while glutamic acid has negative charged side chain. If charge of glutamic acid was essential for the interaction between two residues, this mutation would affect the activity of the enzyme. Lastly, the mutation of E1027 to arginine (E1027R) was generated in order to observe the effect of size and charge of residue. Arginine has a positively charged side chain which is opposite to that of the glutamic acid and its molecular weight is greater than glutamic acid. If size and charge were important for the interaction, this mutation would affect the activity of enzyme.

The effects of R469 mutation on the enzyme activity especially in terms of the acetyl-CoA regulation of the enzyme was also studied since R469 directly binds to acetyl-CoA. Mutation of R469 to serine was invesitgated to examine whether charge would affect the enzyme activity. In addition, mutation of R469 to serine was examined to examine the effect of size on the enzyme activity.

Lastly, D471 directly interacts with acetyl-CoA. Mutation of D471 was investigated to examine the effect of this residue on the acetyl-CoA-dependent pyruvate carboxylation activity.

Since there are many unexpected bands in the purified RePC column from SDS-PAGE analysis for purified wild-type and all mutant RePC except D471At RePC, these bands may be the degraded enzyme. So, further analysis such as western blot analysis probed with the antibody for RePC should have done in order to confirm the hypothesis. If there are the degraded fractions of the enzyme, they may affect the biotin assay and other catalytic activities such as pyruvate carboxylation and ATP cleavage activity.

Because substitution of the above residues of enzyme might affect its secondary, tertiary, and quaternary structures, the examination of the possible

structural changes should be confirmed before performing other experiments. The SDS-PAGE analysis of expression level and solubility of whole cell extracts from wild-type and mutant RePC was examined. The results showed that all mutants of RePC were in soluble form which was similar to the wild-type enzyme; therefore those mutations probably do not affect the gross structure of the enzyme.

In the structure of RePC, R469 interacts with 3'-phosphate and β-phosphate of acetyl-CoA. R469S and R469K mutations resulted in the reduction of acetyl-CoA-dependent pyruvate carboxylation activity and the increase in K_a for acetyl-CoA. Due to the direct interaction between R469 and acetyl-CoA, the mutation of R469 may reduce the acetyl-CoA binding leading to an increase in K_a for acetyl-CoA. The effects of R469K mutation are greater than that of R469S mutation which was similar to mutations R427 and R472 which directly interact with acetyl-CoA (45). R427S and R427K RePC mutants possessed 15- and 76-fold increase in their K_a for acetyl-CoA respectively compared with the wild-type enzyme. Furthermore, R427K mutant affected the cooperativity of the action of acetyl-CoA (45). R472S and R472K RePC exhibited 203- and 252- fold increase in their K_a for acetyl-CoA respectively compared with the wild-type enzyme (45). The greater effects of mutations to lysine were rationalized by the suggestion that mutation of arginine to lysine may still maintain the interaction between residue and acetyl-CoA, however, lysine could not form interaction with other residues in allosteric domain and ultimately disrupted the positioning of acetyl-CoA in the binding site (45). On the other hand, mutation of arginine to serine would destroy the interaction between this residue and acetyl-CoA, but the acetyl-CoA could normally interact with other residues in the binding site (45).

For pyruvate carboxylation activity, mutations of R469 slightly reduced acetyl-CoA dependent enzyme activity similar to those of R427 and R472 mutations. However, R469 mutations increased acetyl-CoA independent pyruvate carboxylation activity (k^0_{cat}) while little changes were observed in R427 and R472 mutations. R469 mutations increased biotin-dependent MgATP cleavage activity both in the presence and absence of acetyl-CoA, but R427 and R472 mutations greatly reduced both k^0_{cat} and k_{cat} for biotin-dependent MgATP cleavage activity. The increase in acetyl-CoA independent pyruvate carboxylation activity and in biotin-dependent MgATP cleavage activity in the presence and absence of acetyl-CoA indicate that mutation of R469 may

remove some constraint of the activity of the enzyme. In the acetyl-CoA bound subunit of RePC, the guanidinium side chain group of R469 and the α-amide of D471 directly interact with acetyl-CoA. R469 also interacts with D471which in turn interacts with T474, and T474 in turn interacts with R1053. However, in the absence of acetyl-CoA, R469 interacts with E360 instead of D471 (see Figure 5.1). This can be described with the less distance between R469 and E360 in acetyl-CoA free subunit (3.49 Å) compared with acetyl-CoA bound subunit (11.12 Å). E360 is located in the BC domain, but it is not directly involved in biotin carboxylation. However, changes in interactions between these residues cannot be exactly interpreted to depend on acetyl-CoA because the structure of RePC is asymmetry both in the presence and absence of acetyl-CoA (52). So, different interactions between residues in the presence and absence of acetyl-CoA may happen due to the asymmetry of RePC tetramer. However, the positions of these residues in RePC in acetyl-CoA bound subunit and acetyl-CoA free subunit cannot be compared because the resolution of RePC subunit without acetyl-CoA is rather low (19, 52).

The studies of SaPC structures in the presence and absence of acetyl-CoA were performed (48). The crystal structure of SaPC is more symmetrical which is different from the crystal structure of RePC. The acetyl-CoA is bound to all four subunits in SaPC with acetyl-CoA. In SaPC, the corresponding residues of R469 and E360 from RePC are S463 and L353 respectively. The positions of S463 and L353 in acetyl-CoA bound subunit are slightly different from positions in acetyl-CoA free subunit. This suggests that positioning of residues in SaPC and corresponding residues in RePC does not depend on acetyl-CoA binding, and the differential positions in RePC are caused by the asymmetry of the tetramer. Interestingly, in SaPC, R1053 which is the corresponding residue of R1059 in RePC directly interacts with acetyl-CoA instead of interacting through T474, D471, and R469. This may suggest that this network interaction between residues in allosteric domain and acetyl-CoA is unique in RePC. The mutation of D471 to alanine had great impact on the acetyl-CoA induced pyruvate carboxylation reaction of RePC though the concentration of acetyl-CoA was up to 250 μM. This may indicate that D471 essentially affects either acetyl-CoA binding and/or its effect on the activity of the enzyme. The network interaction between acetyl-CoA, R469, D471, T474, and R1059 may help positioning of acetyl-

CoA and other residues into the optimal configuration that ultimately promotes catalysis of the enzyme. Mutation of D471 may destroy theses interactions especially with R469 and T474, and leads to miss-positioning of R469 and disturbing the interaction with acetyl-CoA. D471A also reduced the acetyl-CoA independent pyruvate carboxylation activity by approximately 40%. In the subunit without acetyl-CoA of RePC, R469 no longer interacts with D471, but D471 still interacts with T474. The mutation of D471 may further reduce any interaction between D471 and R469 but strengthens its interaction with T474 which may interrupt the interaction between T474 and R1059 in the absence of acetyl-CoA. These finally reduce the activity of the enzyme in the absence of acetyl-CoA.

In the structure of RePC in subunit with acetyl-CoA, E1027 interacts with R472 while the position of E1027 relative to R472 is not clear in the subunit that acetyl-CoA is unbound (19). E1027A slightly reduced in the enzyme activity induced by acetyl-CoA and little increased in K_a for acetyl-CoA. E1027R caused greater reduction in acetyl-CoA induced pyruvate carboxylation activity and increase in K_a for acetyl-CoA than that of E1027A. The mutation of E1027 to arginine may cause repulsion between E1027R and R472 which in turn results in the miss-positioning of R472 in the binding of acetyl-CoA. E1027 mutations also increased in acetyl-CoA independent pyruvate carboxylation activity. Owing to less resolution of the positioning of E1027 and R472 in the absence of acetyl-CoA in RePC, it is difficult to propose the explanation for the increases in acetyl-CoA independent pyruvate carboxylation activity. It is possible that there is the interaction between E1027 and other residues which only occurs in subunit without acetyl-CoA. This interaction may restrain the activity of the enzyme, and it is removed once acetyl-CoA binding to the enzyme causing an increase in acetyl-CoA induced activity of the enzyme. Nevertheless, further studies in the structure of RePC in subunit without acetyl-CoA especially the high resolution study of crystal structure in this subunit are required to clarify this explanation. The mutation E1027A and E1027R greatly increased in biotin-dependent MgATP cleavage both in presence and absence of acetyl-CoA compared to wild-type. The interaction between E1027 and R472 in acetyl-CoA bound subunit of RePC may impose some restriction on the MgATP cleavage reaction. The mutation of E1027 may relief this restriction and increase the activity, however, the enhanced rate

of MgATP cleavage may not be coupled to biotin carboxylation causing not increased rate of the overall pyruvate carboxylation reaction.

Since D1018 only interacts with R427 in the subunit without acetyll-CoA bound, D1018A and D1018R mutations mainly affect acetyl-CoA independent pyruvate carboxylation activity. D1018A possessed a large increase in k^0_{cat} for pyruvate carboxylation, but slightly affected acetyl-CoA dependent activity, Hill coefficient, and K_a of acetyl-CoA activation. In the structure of RePC with acetyl-CoA bound, D1018 is in a great distance from R427 for almost 27 Å (see Figure 5.2), however, the positioning of D1018 in subunit without acetyl-CoA bound is different and close enough to interact with R427. The positioning of R427 in subunit with and without acetyl-CoA bound is also different, but to a lesser degree. On the other hand, the distances between N1012 and R420, which are the corresponding residues in SaPC for D1018 and R427 respectively, are not different and about 26-27 Å in the structures of the tetramer with and without acetyl-CoA bound. This also confirms that the differential positioning of D1018 and R427 is not due to acetyl-CoA binding but rather the asymmetry in RePC tetramer. The mutation of D1018 increased biotin-dependent MgATP cleavage activity both in the presence and absence of acetyl-CoA. The increase in the MgATP cleavage reactions in the absence of acetyl-CoA in D1018A and D1018R may result from the disruption of the interaction between D1018 and R427. This interaction which only occurs in the subunit without acetyl-CoA bound may help the enzyme to restrain the activity and stabilize the enzyme into the inactive form until the acetyl-CoA activation, but mutations reduce this interaction and let the enzyme release the constraint. However, increased MgATP activities cannot be coupled with biotin carboxylation which results in decrease of overall pyruvate carboxylation activities. In the RePC in the subunit with acetyl-CoA bound, the obvious interaction between D1018 and other residues is not found, so the proposed explanation of increased in acetyl-CoA induced MgATP cleavage due to loss of interaction with D1018 cannot be exploited.

In summary, the mutations of R469, D471, E1027 and D1018 (R469S, R469K, D471A, E1027A, E1027R, D1018A, D1018R) of RePC mainly produce two types of results. The first results cause remarkable reduced in pyruvate carboxylation activity by acetyl-CoA (R469S, R469K, D471A, and E1027R) which are

comprehensible that these mutations destroy the acetyl-CoA binding and/or action, either by destroying the direct interaction between the acetyl-CoA and mutated residue or indirectly disrupting the interaction between the acetyl-CoA and other residues in the allosteric domain. The second type results in the increase of acetyl-CoA independent pyruvate carboxylation activity and the biotin-dependent MgATP cleavage both in the presence and absence of acetyl-CoA (R469S, R469K, E1027A, E1027R, D1018A, and D1018R). As mentioned earlier, the differences in the positioning of interactions between residues in the subunit with and without acetyl-CoA bound in RePC are more inclined to result from the asymmetry of tetramer rather than as a result from acetyl-CoA binding. The RePC tetramer that is obviously asymmetry and the enzyme conformation that allows only one pair of subunits to perform the activity can be considered that PC exhibits half-of-the sites reactivity with the interchange of the activity between pair of subunits on opposite faces of the tetramer, and this type of activity has been proposed for the related biotin carboxylase enzyme (44, 53). Even though the tetramer of SaPC is more symmetrical than that of RePC, the asymmetrical tetramer of SaPC can be observed (54). Moreover, the study of cryoelectron microscopy of SaPC tetramer by Tong and co-workers have shown the evidence that the SaPC tetramer undergoes transitions between symmetrical and asymmetrical conformations during the reaction , and there is the alternations between pairs of subunits on opposite faces of the tetramer (55). The differences between the crystal structure of SaPC and RePC probably caused the stabilization of the different tetrameric conformations (55). So, the interactions between residues in the allosteric domain which only occurs in RePC for example, R469 and E360 and R427 and D1018, may enhance this stabilization of the tetrameric conformation. Moreover, due to interchanges between the asymmetrical and symmetrical conformers of SaPC during catalysis (55), some interaction should be removed in order to transform from one conformer to another form. Interaction between R469 and E360 and interaction between R427 and D1018 only occurring in the subunit without acetyl-CoA bound are evident that there is a restriction of the conversion of enzyme from asymmetry to symmetry. Consequently, mutations of these residues reduce these interactions and relax these constraints which allow free transformation between two conformers and cause increase in enzyme activity especially in the absence of acetyl-CoA.

Interestingly, the acetyl-CoA independent activity of SaPC which is more symmetrical than RePC is greater than that of RePC (49). The greater increase in biotin-dependent MgATP cleavage activity both in the absence and presence of acetyl-CoA suggests that the binding of pyruvate to the enzyme also enhance the interchange of the asymmetrical conformer to symmetrical conformer. This reaction is evident to be relevant to the transformation from the asymmetrical conformer to symmetrical conformer in SaPC (55).

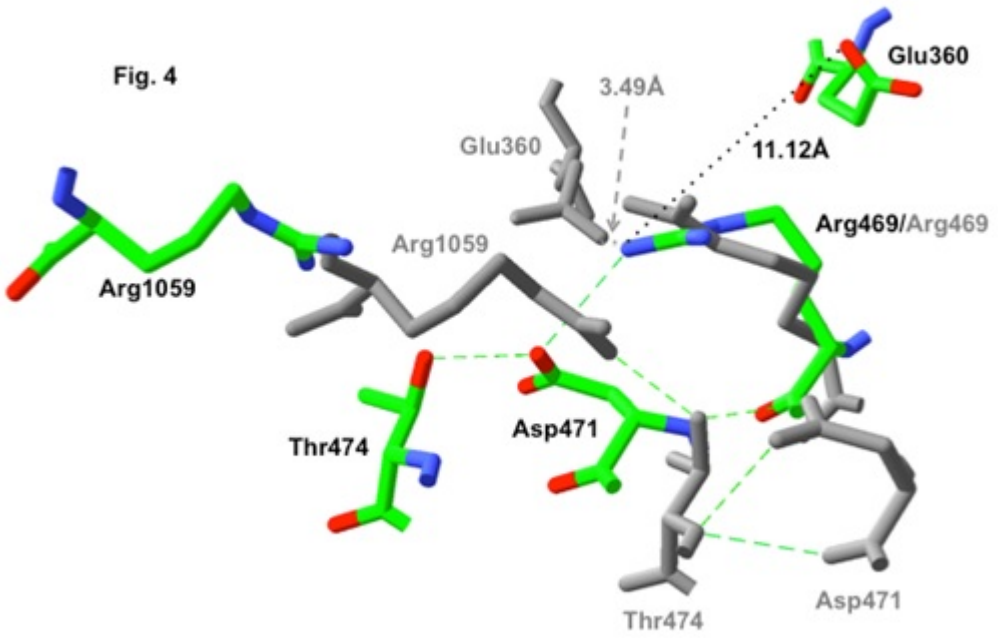

Figure 5.1 Relative positions of Glu360, Arg469, Asp471, Thr474, and Arg1059 residues in the RePC subunit with acetyl-CoA bound (shown in colored residues with black labels) and without acetyl-CoA bound (shown in grey residues with grey labels)

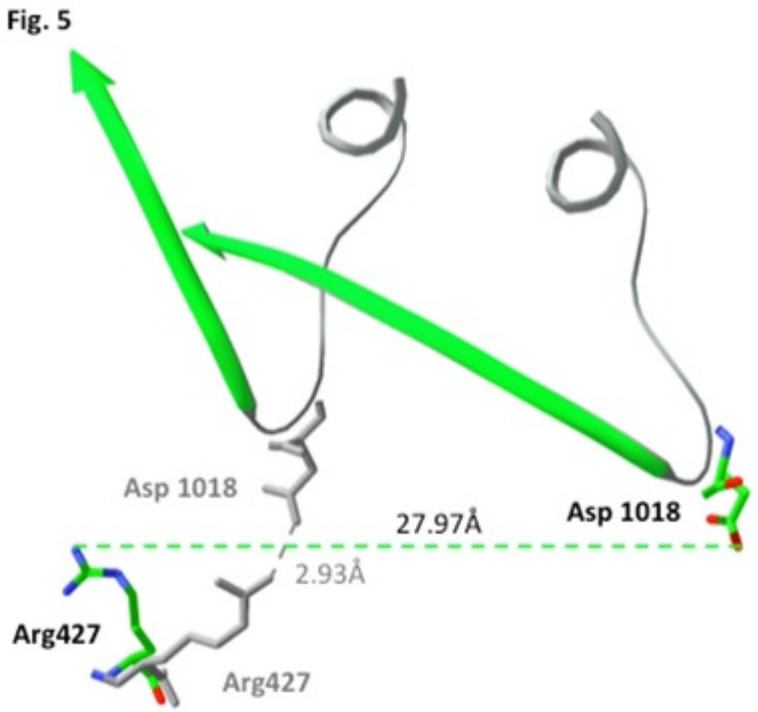

Figure 5.2 Positioning of Arg427 and Glu1018 in the RePC subunit with acetyl-CoA bound (shown in colored residues with black labels) and without acetyl-CoA (shown in grey residues with grey labels)

CHAPTER VI
CONCLUSIONS

1. D1018A, D1018N, D1018R, E1027A, E1027Q, E1027R, R469S, R469K, and D471A RePC were expressed in *E. coli* BL21 (DE3) with bacterial biotin ligase (*birA*) gene and purified.

2. More than 50% of wild-type and D1018A, D1018N, D1018R, E1027A, E1027Q, E1027R, R469S, R469K, and D471A RePC were found in the soluble fraction.

3. R469S and R469K RePC reduced in k_{cat} for acetyl-CoA activated pyruvate carboxylation activity and the binding affinity for acetyl-CoA.

4. D471A RePC completely lost its acetyl-CoA induced pyruvate carboxylation activity, and it also decreased in the catalytic rate of the acetyl-CoA-independent pyruvate carboxylation compared with wild-type RePC.

5. E1027A and E1027R RePC showed the reduction of k_{cat} for acetyl-CoA activated pyruvate carboxylation activity and the binding affinity for acetyl-CoA.

6. R469S, R469K, E1027A, E1027R, D1018A, and D1018R RePC showed increased pyruvate carboxylation activity in the absence of acetyl-CoA and bicarbonate-dependent MgATP cleavage activity both in the presence and absence of acetyl-CoA.

REFERENCES

1. Knowles JR. The mechanism of biotin –dependent enzymes. Annu Rev Biochem. 989; 58:195-221.
2. Melville, D.B., Moyer, A.W., Hofmann, K., and du Vigneaud, V. The structure of biotin: the formation of thiophenevaleric acid from biotin. J. Biol. Chem. 1942; 146: 487-492.
3. Harris, S.A., Wolf, D.E., Mozingo, R., Anderson, R.C., Arth, G.E., Easton, N.R., Heyl, D., Wilson, A.N., and Folkers, K. Biotin. II. Synthesis of biotin. J. Am. Chem. Soc. 1944; 66: 1756- 1757.
4. Owen OE, Kalhan SC, Hanson RW. The key role of anaplerosis and cataplerosis for citric acid cycle function. The Journal of Biological Chemistry. 2002;277: 30409-30412.
5. Jitrapakdee S. and Wallace, J. C., Structure, function and regulation of pyruvate carboxylase. Biochem j, 1999; 370:1-16.
6. Ashworth JM, Kornberg HL. The anaplerotic fixation of carbon dioxide by *Escherichia coli*. Proc R Soc Lond B Biol Sci. 1966; 165: 179-188.
7. Brewster NK, Val DL, Walker ME, Wallace JC. Regulation of pyruvate carboxylase isozyme (PYC1, PYC2) gene expression in *Saccharomyces cerevisiae* during fermentative and nonfermentative growth. Archives of Biochemistry and Biophysics. 1994; 311:62-71.
8. Huet C, Menendez J, Gancedo C, Francois JM. Regulation of pyc1 encoding pyruvate carboxylase Isozyme I by nitrogen sources in *Saccharomyces cerevisiae*. European Journal of Biochemistry / FEBS. 2000;267:6817-6823.
9. Jitrapakdee, S., St Mourice. M., Cleland, W. W., Rayment, I., Wallace, J. C. and Attwood, P. V. Structrue, mechanism and regulation of pyruvate carboxylase. Biochem J. 2008; 413: 369-387.

10. Ashman, L.K. and Keech, D.B. Sheep kidney pyruvate carboxylase. Studies on the coupling of Adenosine triphosphate hydrolysis and CO_2 fixation. J. Biol. Chem. 1975; 250: 14-21.

11. Kaziro, Y., Hass, L.F., Boyer, P.D., and Ochoa, S. Mechanism of the propionyl carboxylase reaction. II. Isotopic exchange and tracer experiments. J. Biol. Chem. 1952; 237: 1460-1468.

12. Ogita, T. and Knowles, J.R. On the intermediacy of carboxyphosphate in biotin-dependent carboxylations. Biochem. 1988; 27: 8028-8033.

13. Attwood, P.V. The structure and the mechanism of action of pyruvate carboxylase. Int. J. Biochem.Cell Biol. 1995; 27:231-249.

14. Attwood, P.V., Tipton, P.A., and Cleland, W.W. Carbon-13 and deuterium isotope effects on oxaloacetate decarboxylation by pyruvate carboxylase. Biochem. 1986; 25; 8197-8205.

15. Tipton, P.A. and Cleland, W.W. Carbon-13 and deuterium isotope effects on the catalytic reaction of Biotin carboxylase. Biochem. 1988; 27: 4325-4331.

16. Jitrapakdee, S., Booker, G. W., Cassady, A. I. and Wallace, J. C. Cloning, sequencing and expression of rat liver pyruvate carboxylase. Biochem. J. 19996; 316:631-637.

17. Waldrop, G. L., Rayment, I. and Holden, H.M. Three-dimensional structure of the biotin carboxylase subunit of acetyl CoA carboxylase. Biochemistry. 1994; 33: 10249-10256.

18. Kazuta, Y., Tokunaga, E., Aramaki, E. and Kondo, H. Identification of lysine-238 of *Escherichia coli* biotin carboxylase as an ATP-binding residue. FEBS Lett. 1998; 427: 377-380.

19. St Maurice, M., Reinhardt, L., Surinya, K. H., Attwood, P. V., Wallace, J. C., Cleland, W.W. and Rayment, I. Domain architecture of pyruvate carboxylase, a biotin-dependent multifunctional enzyme. Science 2007; 317: 1076-1079.

20. Attwood, P. V. and Cleland, W.W. Decarboxylation of oxaloacetate by pyruvate carboxylase. Biochem. 1986; 25: 8191-8196.

21. Hall, P. R., Zheng, R., Antony, L., Pusztai-Carey, M., Carey, P.R. and Yee, V.C. Transcarboxylase 5S structures: assembly and catalytic mechanism of a multienzyme complex. EMBO J.2004; 23: 3621-3631.

22. Yong-Biao, J., Islam, M. N., Sueda, S. and Kondo, H. Idenfication of the catalytic residues involved in the carboxyl transfer of pyruvate carboxylase. Biochemistry 2004; 43: 5912-5920.

23. Zeczycki T.N., St Maurice M., Jitrapakdee S., Wallace J.C., Attwood P.V., Cleland W.W. Insight into the carboxyl transferase domain mechanism of pyruvate carboxylase from *Rhizobium etli*. Biochemistry 2009; 48: 4305-4313.

24. Duangpan S, Jitrapakdee S, Adina-Zada A, Byrne L, Zeczycki TN, Stt Maurice M, et al. Probing the catalytic roles of Arg548 and Gln 552 in the carboxyl transferase domain of the *Rhizobium etli* pyruvate carboxylase by site-directed mutagenesis. Biochemistry 2010; 49:3296-3304.

25. Barden, R. E., Taylor, B. L., Isohashi, F., Frey, W.H., Lee, J.C., Zander, G. and Utter, m.F. Structural properties of pyruvate carboxylases from chicken liver and other sources. Proc. Natl. Acad. Sce. USA. 1975; 72:4308-4312.

26. Mukhopadhyay, B., Stoddard, S.F. and Wolfe, R.S. Purification, regulation and biochemical characterization of pyruvate carboxylase from *Methanobacterium thermoautotrophicum*strains ΔH. J. Biol. Chem. 1998; 273:5155-5166.

27. Mukhopadhyay, B., Patel, V.J. and Wolfe, R.S. A stable arcahel pyruvate carboxylase from the hyperthermophile *Methanococcus jannaschii*. Arch. Microbiol. 2000; 174: 406-414.

28. Kondo, S., Nakjima, y., Sugio, S., yong-Biao, J., Sueda, S. and Kondo, H. Structure of the biotin carboxylase subunit of pyruvate subunit of pyruvate carboxylase from Aquifex aeolicus at 2.2 A° resolution. Acta Crystallogr. Sect. D Biol. Crystallogr. 2004; 60: 486-492.

29. Goss, J. A., Cohen, N. D. and Utter, M. F. Characterization of the subunit structure of pyruvate carboxylase from *Pseudomonas citronellolis*. J. Biol. Chem. 1981; 256: 11819-11825.

30. Lai, H., Kraszewski, J. L., Parwantini, E. and Mukhopadhyay, B. Identification of pyruvate carboxylase genes in *Pseudomonas aeruginosa* PAO1 and development of a *P. aeruginosa* –based overexpression system for α4- and α4β4- type pyruvate carboxylase. Appl. Environ. Microbiol. 2006; 72:7785-7792.

31. Islam, M. N., Sueda, S. and Kondo, H. Construction of new forms of pyruvate carboxylase to assess the allosteric regulation by acetyl CoA. Protein Eng. Des. Sel. 2005; 18:71-78.

32. Attwood PV. Locus of action of acetyl coA in the biotin-carboxylation reaction of pyruvate carboxylase. Biochemistry. 1993; 32:12736-42.

33. Attwood PV, Graneri BD. Bicarbonate-dependent ATP cleavage catalyzed by pyruvate carboxylase in the absence of pyruvate. The Biochemical Journal. 1992; 287:10117.

34. Branson JP, Nezic M, Wallace JC, Attwood PV. Kinetic characterization of yeast pyruvate carboxylase isozyme pyc 1. Biochemistry. 2002; 41:4459-4466.

35. Legge GB, branson JP, Attwood PV. Effects of acetyl CoA on the pre-steady-state kinetics of the biotin carboxylation reaction of pyruvate carboxylase. Biochemistry. 1996; 35:3849-3856.

36. Scrutton MC, Keech DB, Utter MF. pyruvate carboxylase. iv. partial reactions and the locus of activation by acetyl coenzyme A. The Journal of Biological Chemistry. 1965;240:574-81.

37. Attwood PV, Wallace JC. The carboxybiotin complex of chicken liver pyruvate carboxylase. A kinetic analysis of the effects of acetyl-CoA, Mg^{2+} ions and temperature on its stability and on its reaction with 2-oxobutyrate. The Biochemical Journal. 1986; 235:359-364.

38. Geeves MA, Branson JP, Attwood PV. Kinetics of nucleotide binding to pyruvate carboxylase.Biochemistry. 1995;37:11846-11854.

39. Adina-Aada A, Jitrapakdee S, Surinya KH, Melldoie MJ, Piggott MJ, Cleland WW, et al. Insights intothe mechanism and regulation of pyruvate carboxylase by characterization of a biotin-deficient mutant of the Bacillus thermodenitrificans enzyme. The International Journal of Biochemistry & Cell Biology. 2008; 40:1743-1752.

40. Studer, R., Dahinden, P., Wang, W.W., Auchli, Y., Li, X.D. and Dimroth, P. Crystal structure of the carboxyltransferase domain of the oxaloacetate decarboxylase Na + pump from *Vibrio cholera*. J Mol Biol. 2006; 367:547-557.

41. Kondo, S., Nakajima, Y., Sugio, S., Sueda, S., Islam, M. N. and Kondo, H. Structure of the biotin carboxylase domain of pyruvate carboxylase from Bacillus thermodenitrificans. Acta Crystallogr. Sect. D Biol. Crystallogr. 2006; 63:885-890.

42. Thoden, J. B., Blanchard, C. Z., Holden, H. M. and Waldrop, G. L. Movement of the biotin carboxylase B-domain as a result of ATP binding. J. Biol. Chem. 2000; 275:16183-16190.

43. Sueda S, Islam MN, Kondo H. Protein engineering of pyruvate carboxylase: investigation on the function of acetyl-CoA and the quaternary structure. European Journal of Biochemistry / FEBS. 2004; 271:1391-1400.

44. Janiyani K, Bordelon T, Waldrop GL, Cronan JE, Jr. Function of Eschericia coli biotin carboxylase requires catalytic activity of both subunits of the homodimer. J Biol Chem. 2001; 276:29864-29870.

45. Adina-Zada A, Sereeruk C, Jitrapakdee S, Zeczycki T.N., St. Maurice M, Wallace JC, and Attwood PV. The roles of Arg427 and Arg472 in the binding and allosteric effects of acetyl CoA in pyruvate carboxylase. Biochemistry. 2012; 51(41): 8208-8217.

46. Adina-Zada A., Zeczycke, T.N., Attwood P.V. Regulation of the structure and activity of pyruvate carboxylase by acetyl-CoA. Arch. Biochem. Biophys. 2011.

47. Attwood P.V., W. Johannssen et al. The existence of multiple tetrameric conformers of chicken liver pyruvate carboxylase and their roles in dilution inactivation. Biochem J. 1993; 290: 583-590.

48. Xiang, S. and Tong, L., Crystal structures of human and *Straphylococcus aureus* pyruvate carboxylase and molecular insights into the carboxyltransfer reaction. Nat Struct Mol Biol. 2008; 15:295-302.

49. Linda, P. C., Xiang, S., Lasso, G., Gil, D., Valle, M. and Tong, L. A symmetrical tetramer for *S. aureus* pyruvate carboxylase in complex with coenzyme A. 2009; 17: 823-832.

50. Athappily, F.K. and Hendrickson, W.A. Structure of the biotinyl domain of acetyl CoA carboxylase determined by MAD phasing. Structure. 1995; 3: 1407-1419.

51. Roberts, E.L., Shu, N., Howard, M.J., Broadhurst, R.W., Chapman-Smith, A., Wallace, J.C., Morris, T., Cronan, Jr, J.E. and Perham, R.N. Solution structures of apo- and holo-biotinyl domains from acetyl coenzyme A carboxylase of Escherichia coli determined by triple-resonance NMR spectroscopy. Biochemistry. 1999; 38, 5045-5053.

52. Lietzan, A.D., Menefee, A.L., Zeczycki, T. N., Kumar, S., Attwood, P. V., Wallace, J. C., Cleland, W. W., and St Maurice, M. Interaction between the biotin carboxyl carrier domain and the biotin carboxylase domain in pyruvate carboxylase from *Rhizobium etli*. Biochemistry. 2011; 50, 9708-9723.

53. de Queiroz, M.S., and Waldrop, G. L. Modeling and numerical simulation of biotin carboxylase kinetics: implications for half-sites reactivity. Journal of theoretical biology. 2007; 246, 167-175.

54. Lasso, G., Yu, L. P., Gil, D., Xiang, S., Tong, L., and Valle, M. Cryo-EM analysis reveals new Insights into the mechanism of action of pyruvate carboxylase. Structure. 2010; 18,1300-1310.

55. Lasso, G., Yu, L. P., Gil, D., Lazaro, M., Tong, L., and Valle, M. Functional conformations for Pyruvate carboxylase during catalysis explored by cryoelectron microscopy. Structure.2014; 22(6), 911-922.

BIOGRAPHY

NAME	Miss Kamonman Choosangtong
DATE OF BIRTH	28th December 1985
PLACE OF BIRTH	Bangkok, Thailand
INSTITUTIONS ATTENDED	Mahidol University, 2004-2008: Bachelor of Science (Biochemistry) Mahidol University, 2010-2015: Master of Science (Biochemistry)
HOME ADDRESS	395 Sukhumvit 77, Suan Luang, Bangkok, Thailand kamonman.c@hotmail.com

PUBLICATION

Choosangtong K, Sirithanakorn C, Adina-Zada, A., Wallace, J.C., Jitrapakdee S, and Attwood, P.V. Residues in the acetyl CoA binding site of pyruvate carboxylase involved in allosteric regulation. FEBS Lett. 2015; 589(16), 2073-2079.